ARL-TR-9925 ● JUNE 2024

Atmospheric Intelligence for Hybrid Power Advancements: Volume 3 (Whole Sky Image Percent Cloud and Blue Sky Analyses)

by Gail Vaucher, Jarrod LaRosa, Michael Lee, and Robert Jane

NOTICES

Disclaimers

The findings in this report are not to be construed as an official Department of the Army position unless so designated by other authorized documents.

Citation of manufacturer's or trade names does not constitute an official endorsement or approval of the use thereof.

Destroy this report when it is no longer needed. Do not return it to the originator.

ARL-TR-9925 ● JUNE 2024

Atmospheric Intelligence for Hybrid Power Advancements: Volume 3 (Whole Sky Image Percent Cloud and Blue Sky Analyses)

Gail Vaucher, Michael Lee, and Robert Jane
DEVCOM Army Research Laboratory

Jarrod LaRosa
Virginia Military Institute

REPORT DOCUMENTATION PAGE

1. REPORT DATE	2. REPORT TYPE	3. DATES COVERED	
		START DATE	END DATE
June 2024	Technical Report	7/01/2023	12/30/2023

4. TITLE AND SUBTITLE
Atmospheric Intelligence for Hybrid Power Advancements: Volume 3 (Whole Sky Image Percent Cloud and Blue Sky Analyses)

5a. CONTRACT NUMBER	5b. GRANT NUMBER	5c. PROGRAM ELEMENT NUMBER
5d. PROJECT NUMBER	**5e. TASK NUMBER**	**5f. WORK UNIT NUMBER**

6. AUTHOR(S)
Gail Vaucher, Jarrod LaRosa, Michael Lee, and Robert Jane

7. PERFORMING ORGANIZATION NAME(S) AND ADDRESS(ES)	8. PERFORMING ORGANIZATION REPORT NUMBER
DEVCOM Army Research Laboratory ATTN: FCDD-RLA-ID White Sands Missile Range, NM 88002	ARL-TR-9925

9. SPONSORING/MONITORING AGENCY NAME(S) AND ADDRESS(ES)	10. SPONSOR/MONITOR'S ACRONYM(S)	11. SPONSOR/MONITOR'S REPORT NUMBER(S)

12. DISTRIBUTION/AVAILABILITY STATEMENT
DISTRIBUTION STATEMENT A. Approved for public release: distribution unlimited.

13. SUPPLEMENTARY NOTES
ORCID: Michael Lee, 0000-0002-0419-6069

14. ABSTRACT
This report documents a blue sky algorithm milestone used in the process of converting whole sky imagery into informative quantities needed to calculate surface layer irradiance. Power resource diversity is critical in maintaining future reliable and consistent electrical flow. Forecasting power generation is key in managing and optimizing multiple resources. Photovoltaic (PV) technology is an energy source that is ready for this hybridized power strategy. PV power is a function of irradiance. Primary irradiance inhibitors are atmospheric clouds. A Whole Sky Imager (WSI) visually captures clouds and can quantify power production impacts. Earlier research defined sky type using a red–green–blue thresholding method. Nonlinear correlations led to a hue–saturation–value method that highlights blue sky pixels. This approach was applied to ground objects and led us to determine that image artifacts represent <3% of the total pixel count. Comparing calculated cloud cover to sky observer values, overcast cases showed good agreement. Clear cases were within a 3% difference, reinforcing artifact challenges. Partly cloudy cases produced favorable results. All WSI image elements were tallied and cross-checked against the WSI pixel total. Results were well within acceptable levels. This research improved WSI analysis capabilities, producing algorithms poised for applications that will ultimately reduce Warfighter vulnerabilities/delayed disaster relief recoveries.

15. SUBJECT TERMS
hybridize power; photovoltaic; PV; solar radiation; Whole Sky Imager; whole sky images; image analysis; percent blue sky; percent cloud cover; percent sun disc; Energy Sciences; Military Information Sciences; Network, Cyber, and Computational Sciences

16. SECURITY CLASSIFICATION OF:			17. LIMITATION OF ABSTRACT	18. NUMBER OF PAGES
a. REPORT	b. ABSTRACT	C. THIS PAGE		
UNCLASSIFIED	UNCLASSIFIED	UNCLASSIFIED	UU	57

19a. NAME OF RESPONSIBLE PERSON	19b. PHONE NUMBER *(Include area code)*
Gail Vaucher	(575) 678-3237

STANDARD FORM 298 (REV. 5/2020)
Prescribed by ANSI Std. Z39.18

Contents

List of Figures

List of Tables

Acknowledgments

The authors wish to thank Mr Sean D'Arcy for providing the 15 cases of simulated Whole Sky Imager data and the Army Test and Evaluation Command's Meteorology Department for their field site support with the US Army Combat Capabilities Development Command Army Research Laboratory research photovoltaic power testbed. Appreciation is extended to John Raby for his consistently excellent technical review. Finally, special thanks go to the Technical Publishing Branch for its high-quality technical editing, specifically to Technical Editor, Jovina Allen and Team Lead, Jessica Schultheis.

Executive Summary

Future tactical and civilian electrical power will be strengthened by using a diversity of power resources to maintain a reliable and consistent flow of electricity. A foreknowledge of potential energy contributions is critical to the successful management and optimization of these multiple power resources. Photovoltaic (PV) technology is one renewable energy process that is ready and able to participate in this hybridized power strategy. PV power is primarily a function of solar radiation and panel temperature. Focusing on irradiance, energy from the sun enters the top of the atmosphere and travels down to the PV panel mounted at the earth's surface. The greatest irradiance inhibitors are shadows, primarily atmospheric clouds. Quantifying this effect can be done by determining the percent of cloud cover filtering the solar radiation. A Whole Sky Imager (WSI) documents clouds in a visual photo of the sky stretching from horizon to horizon. Refining the analysis and quantification of cloud cover from WSI images was central to this research.

Earlier US Army Combat Capabilities Development Command (DEVCOM) Army Research Laboratory (ARL) research defined an algorithm that determined the sky type based on the solar disc size, using a red–green–blue (RGB) thresholding method. The non-linear correlations between sky type and solar disc size led to the pursuit of a second image analysis method to refine the initial mixed results. Beginning with a review of professional cloud quantification techniques, researchers discovered a subsequent procedure using a hue–saturation–value (HSV) method to highlight the WSI blue sky pixels. This effective approach was applied to masking user-identified, non-cloud, and ground objects, also referred to as artifacts. The result was a stationary non-cloud-object-masking algorithm that was added to the WSI analysis.

An HSV blue sky algorithm was developed to calculate the cloud cover by interpreting all non-blue-sky pixels as clouds. Having determined that the sun's corona and image artifact features represented less than 3% of the total pixel count, the calculated cloud cover was compared to the (human) sky observer values.

- Overcast (OVC) cases showed good agreement between observer and calculated cloud cover.
- Clear (CLR) cases were within a 3% difference, re-enforcing the ongoing challenges in interpreting artifacts appearing like clouds, and horizon "noise."
- Partly cloudy (PC) cases produced favorable results with the inclusion of mid-point selection (30% ➔ 40% = 35%) options for the observer's values.

A tally of all WSI image elements was cross-checked against the full WSI pixel total. Results showed 60% of the OVC cases matched the total pixel count, with a total pixel excess of no more than 0.3% in the balance of cases. The CLR cases showed a consistent trend of overlapping pixel counts, between 0.3% and 0.5%. The PC case results ranged between 0 (perfect match) and 0.9% (pixel duplication). Based on the accepted 3% buffer for representing artifacts, ground silhouettes, and so forth, these findings were well within acceptable levels.

In conclusion, the research conducted has improved whole sky image analysis capabilities by accounting for all the major elements within the WSI images. The algorithms developed are poised for their application in preparing data for the solar radiation model input. As the process becomes more precise and accurate, the ability to integrate solar fuels into the hybridized tactical and civilian power resources will improve, thus reducing Warfighter vulnerabilities to enemy forces or delayed recoveries in disaster relief emergencies. In short, this report documents a significant blue sky algorithm milestone used in the process of converting whole sky imagery into informative quantities needed to calculate surface layer solar radiation.

1. Introduction

This report documents a significant milestone in the process of converting whole sky imagery into informative quantities needed to calculate surface layer solar radiation. To review the foundational research upon which this phase of the investigation is built, see Section 2.

1.1 The Research Problem

Future tactical and civilian electrical power will be strengthened by using a diversity of resources to maintain a reliable and consistent flow of electricity. Managing and optimizing these multiple resources relies on a foreknowledge of their potential contributions. Producing electricity from photovoltaic (PV) technologies is one renewable energy process that is ready and able to contribute to this hybridized power strategy.

PV power potential is primarily a function of solar radiation and panel temperature. Solar radiation photons striking the PV panels determines the maximum potential magnitude of electricity generated by the PV panel. The panel temperature steers the efficiency of production, with cooler temperatures showing greater efficiency (Vaucher et al. 2022).

Focusing on solar radiation, energy from the sun enters the top of the atmosphere and travels down to the PV panel mounted on the earth's surface. As the radiation traverses from space to the surface, it is reflected, absorbed, and transmitted through each atmospheric layer. For details of the radiation transmission process, see Vaucher et al. (2019). The greatest natural inhibitors of the irradiance reaching the PV panel are shadows, with the paramount shadow source being atmospheric clouds. Quantifying this effect can be done by determining the percent of cloud cover filling the dome of sky through which the solar radiation is traveling. One sensor that documents clouds in the sky is the Whole Sky Imager (WSI). This surface sensor generates a 360°, visual map of the sky dome from horizon to horizon. More information on the sensor is found in Section 1.2.

Refining the analysis and quantification of cloud cover from WSI images was the first part of this research. Applying the results was its complement (see Section 4). In Sections 1.2–1.5, a brief review of data resources, atmospheric definitions and observation methods, and the foundational research prompting this work are described.

1.2 Data Resources

The primary data resource for this research was a WSI, which consisted of a digital camera with a fisheye lens. Although most WSI sensors include a physical occulter to block the sun disc, the study's "simulated" WSI device was able to accommodate the potential overexposure caused by the sunlight, through the WSI's internal camera functions. Note that, hereafter, the simulated WSI will be labeled "WSI," unless otherwise indicated.

The WSI images documented sky objects located from the horizon (on all sides) to zenith (straight overhead). As demonstrated in Fig. 1, the circular perimeter aligns with the north–south–east–west horizons and includes a zenith point at the image center. Specific to Fig. 1, the surface-to-space view positions the sun west of zenith. All visible clouds (white and gray) are on the western horizons.

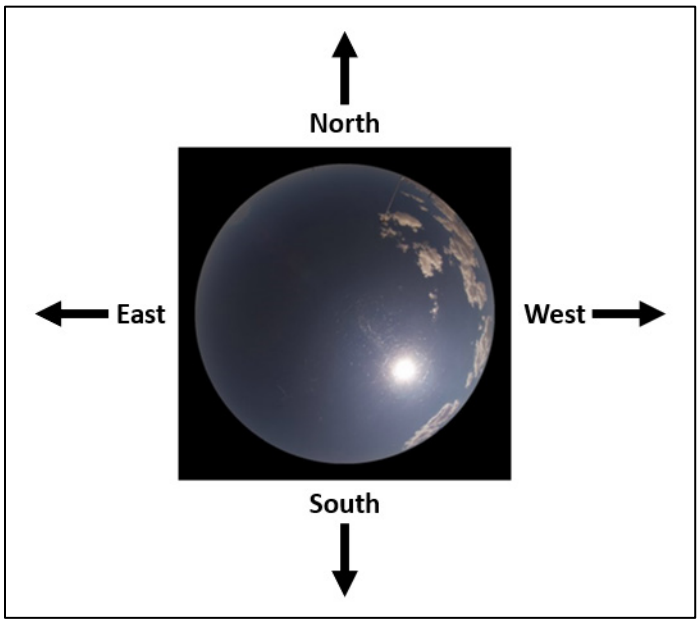

Fig. 1 WSI image examples from 2021 September 14, 1500 MDT

The WSI images were sampled every 15 min, at the same location in Southwestern New Mexico. Although images were acquired from sunrise–twilight to sundown–twilight, we extracted photos that represented the sky between 1000 and 1600 MDT only, to help minimize optical artifacts. The digital camera images were stored in a .jpg (a.k.a., jpeg) format.

For consistency, we used the same 15 days of data selected for the sun-corona study (Vaucher et al. 2023). Table 1 (Vaucher et al. 2023) tabulates these 15 days of raw image data, using a color-coded pattern for the sky type they represent (which will be explained in Section 1.4.1). Here, CLR indicates clear sky; OVC represents

overcast; and PC references partly cloudy sky conditions. When sampled images were absent, time periods were reduced accordingly (i.e., 2021 September 2). To view the actual 1300 MDT images for each day tabulated, see Appendix A.

Table 1 WSI images used for cloud algorithm development

Date (YYMMDD)	Time range (MDT)	Sky type
210826	1000–1600	CLR
210910	1000–1600	CLR
210914	1000–1600	CLR
210917	1000–1500	CLR
210921	1000–1600	CLR
210813	1000–1600	OVC
210814	1000–1600	OVC
210902	1200–1600	OVC
210905	1000–1600	OVC
210925	1000–1600	OVC
210812	1000–1600	PC
210821	1100–1600	PC
210927	1000–1600	PC
211001	1100–1600	PC
211006	1000–1600	PC

1.3 Cloud Types

Identifying the cloud type or cloud layer is part of the solar radiation model input requirements. Cloud classification is defined as "a scheme of distinguishing and grouping clouds according to their appearance, and, where possible, to their process of formation" (American Meteorological Society n.d.). In 1803, Luke Howard established a cloud classifying scheme based on five main factors: genera, species, variety, supplementary features, and mother clouds (American Meteorological Society n.d.). His categorization was later adopted by the World Meteorological Organization. The genera describe the general cloud characteristics in terms of the form (the cloud's basic type)—cumulus, stratus, and cirrus.* The second through fifth factors detail the cloud variety with respect to its shape, structure, arrangement, and transparency. For this study, three basic tropospheric layers and their associated cloud types were used:

- lower (cumulus),

* Although standard stratus clouds are associated with mid-atmospheric levels, this extended flat-layered cloud can be found on all levels; thus, it can be labeled with two names, such as cirrostratus or stratocumulus.

- middle (stratus), and
- top (cirrus) levels.

For a summary of the National Weather Service cloud types, their distance above-ground level, and their appearance, see National Weather Service (2020). The filtering aspects of the cloud types with respect to quantifying surface solar radiation are described in Vaucher et al. (2023).

1.4 Methods of Quantifying Cloud Cover

When the cloud type is defined, it can also establish the cloud layer that filters the radiation as it travels from space to the earth's surface. Quantifying the distribution of these clouds across the sky dome enables one to determine the net effects of incoming direct and diffuse solar radiation potentially reaching the ground. Each cloud has a unique size and fractal shape. Reducing these attributes into a numerical representation is not trivial. Fortunately, meteorologists have two effective approaches for this goal: one method perceives the sky dome in tenths, and the other method uses subdivisions of eighths.

1.4.1 Quantifying Cloudage in Tenths

Referencing the Naval Education and Training Command's manual (Weldon 1985), the following methods are executed to determine the total sky cover in tenths:

1) The observer mentally divides the sky into halves or quarters and estimates the amount of clouds in each section. Each cloud layer amount is estimated by presuming the clouds present in the layer are brought together into a continuous sheet. A tally of all subdivisions produces the determination of total sky cover in tenths.
2) Nighttime cloud observations are determined by the visibility of stars. When the stars do not appear dimmed, the sky is clear. A clear challenge for night observers is discerning the presence of clouds in an area of weakly shining stars from the presence of the milky way.

For the US National Weather Service, the results are communicated using five standard sky cover descriptives:

1) Clear Sky (CLR): Clear sky indicates that there are no clouds or other obscuring aerosols (smoke, fog, haze, etc.) present.

2) Scattered (SCT): SCT conditions indicate a trace of clouds through 5/10 sky cover. (When an isolated cloud is in the lowest layer, with no other clouds present, it is called a "trace" of cloud.)

3) Broken (BKN): BKN sky ranges from 6/10 to 9/10 cloud cover. If there are more than 9/10 but not 10/10, the report entry is "BKN."

4) Overcast (OVC): OVC conditions include 10/10 sky cover.

5) Surface-based obscuring phenomena (X): Examples of surface-based obscuring phenomena include fog, haze, and smoke.

For this study, the observer was trained using 1) a white paper plate that was divided into 10 parts or "pie" slices and 2) a red paper plate that represented the whole sky. The trainee was given multiple cases of random slices scattered across the red plate to determine the percentage of cloud cover. Results were checked by counting the "slices" on the plate.

Although the portion of sky covered with clouds is generally measured in tenths of sky cover, an equally valid method is to portion the observed results in eighths. For this study, we used tenths.

1.4.1 Quantifying Cloudage in Eighths

The World Meteorological Organization leans toward the sky measurements in eights. There are several methods for an observer to deduce this proportioned quantity. The *Global Learning and Observations to Benefit the Environment* (The GLOBE Program n.d.) approach estimates clouds over in quadrants of the sky, and it averages the quadrants. One of the more intriguing approaches, which also aligns with the original WSI analysis concept, was the following (SSERC 2021):

1) The observer uses a square mirror, draws a 4 × 4 grid on the mirror, and lays the mirror on the ground.

2) Using the 16-box grid, the observer counts the squares containing the reflection of the clouds.

3) To reduce the measurements into eighths, the total count (×/16) is multiplied by 2/2, or simply divide the total cloud-reflecting grid count by 2. When the result is a fraction, the results are rounded up.

For example, if seven boxes show clouds, that means there are 7/16 boxes with clouds ➔ 7/16 *2/2 = 3.5/8 grids ➔ 4/8 grid (50% in tenths). Converting between these two systems is demonstrated (see Table 2), using an assimilation of tabulated materials from the *Quartermaster 3* (Weldon 1985).

Table 2 Converting between 10th and 8th cloud cover

Tenths (%)	Eighths (oktas)	Sky label
0	0	CLR
1 or less, but not 0	1 or less, but not 0	SCT (trace)
2 and 3	2	SCT
4	3	SCT
5	4	SCT
6	5	BKN
7 and 8	6	BKN
9 or more, but not 10	7 or more, but not 8	BKN
10	8	OVC
Sky obscured	Sky obscured	X

Finally, it should be noted that standard meteorological sky observation method used at airports documents the sky for the perspective of an aircraft's application. That is, from the top looking downward to the surface. For this application, the cloud cover was perceived from the earth surface upward, with the intent of quantifying the filtering effects of incoming solar radiation.

1.5 Basic Image Analysis

Interpreting an image comes relatively easy for the human brain, due to its perception skills and foreknowledge of what these objects look like. Identifying such attributes via a digital image analysis, however, is much more challenging. Some standard processes are available to initiate the analysis. For example, digital image processing can perform "white balance." That is, there are functions that can remove distorted color casts, so an object that is known to be white to the human eye can be calibrated back to its white color, and the remaining non-white colors in the image are then adjusted or calibrated to the white balance selection. Fair weather cumulus clouds are an example of objects that are generally white to the human eye (Image Engineering 2022).

1.5.1 Optical Artifacts in a WSI Image

Imaging effects that are not easily processed include adapting to visible light as a function of how many atmospheres the sun's rays have traversed, lens distortions, and optical artifacts. Optical artifacts are common to a fisheye lens especially when viewing an unfiltered bright object such as the sun. The resulting unwanted lens flares, glare, and so on can be minimized by sampling images when the sun angle does not reflect off of the opposing dome-shaped glass or lens. For the image analysis phase of this research, the artifacts were reduced by using WSI image samples between 1000 and 1600 MDT, in the fall season.

1.5.2 Corona and Sun Disc Shapes

Lens flaws exaggerated the intense solar disc, creating a corona-like feature around the sun disc perimeter. The pixel magnitudes so closely aligned with the character of the sun disc that it was resolved to include the sun corona pixels when tallying the sun disc.

To the human eye, the solar disc appears to be round. Digitally, the WSI shows the sun to be slightly oval in the morning and evening time periods. The minimum digital disc diameter (nearly round) occurs around solar noon (1300 MDT, for the study cases). Consequently, to minimize solar disc distortion, the 1300 MDT (1200 MST) solar noon images were extracted for algorithm development. Figure 2 demonstrates the solar position at 1300 MDT under clear skies. Note that the fuzzy perimeter appearing as a sun corona.

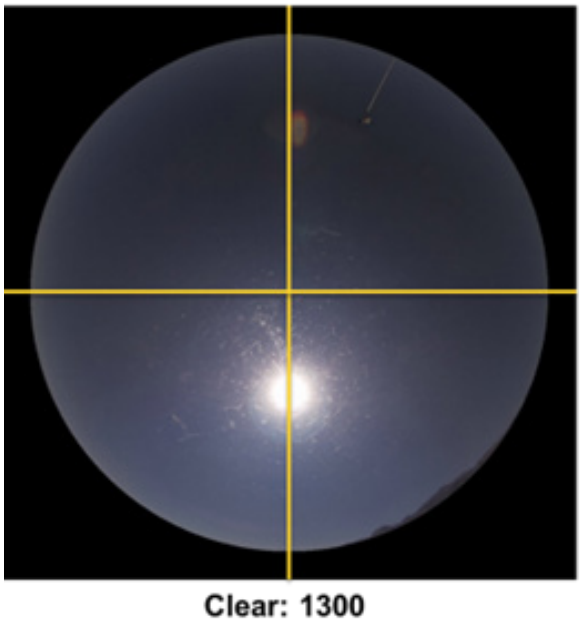

Fig. 2 The sun is close to zenith at 1300 MDT

The previous study (Vaucher et al. 2023) found that the red, green, and blue (RGB) image analysis technique was able to distinguish the solar disc object from all the other image features and imply the sky type. During this subsequent investigation, it was discovered that using the hue, saturation, and value (HSV) thresholding distinguished the blue sky. Before elaborating on the application of these processes, an overview of each image analysis technique is provided.

1.5.3 RGB Thresholding

The RGB color space defines color as the percentage of RGB mixed together. In the Vaucher et al. (2023) study, which determined a correlation between solar disc and sky type, the RGB thresholding technique was used. This RGB technique split the digital image into RGB frequency planes. The digital color image was presented as an 8-bit color; consequently, there were 2^8 or 256 variations with each primary color. Combining these three colors (RGB) generated over 16.6 million possible colors ranging from black (0, 0, 0) through white (255, 255, 255). Extracting or enhancing key elements or objects within the image was largely trial and error. However, with clouds as the primary target, the focus was on the red frequency plane. The current study's application of the RGB threshold implementation is summarized in Section 3 (The MathWorks, Inc 2024).

1.5.4 HSV Thresholding

The HSV color model describes colors by their hue (shade of color), saturation (amount of gray or pure color), and luminance (intensity or overall brightness). The HSV results tend to align more closely with how the human eye perceives color. For example, the hue (H) number corresponds to the color position on a color wheel. When H increases, the colors transition from shades of red to shades of orange, yellow, green, cyan, blue, magenta, and back to red. When H = 0 or 1, they both represent red.

The saturation (S) number indicates the amount of hue or departure from neutral. When S increases, colors vary from unsaturated (gray shades) to fully saturated (no white component). Thus, capturing the purity of the color.

The value (V) element is the maximum value among the RGB components of a specific color. As V increases, the colors become brighter, or more intense, to the eye (The MathWorks, Inc 2024).

2. WSI Image Analysis: Background

The quest to convert the WSI image into informative solar radiation model input began with empirical and machine learning evaluations of WSI images and PV power production. Due to the significant number of images required for the machine learning method, a study was conducted to determine the best image compression techniques for preserving images. The investigation found that the best compression method was a function of the image's application(s) (see Vaucher et al. 2021).

The initial WSI image analysis used a trained meteorologist to categorize the many images into three basic sky types: CLR, PC, and OVC.

- CLR sky images include cloud cover <10%; with the sun not covered.
- OVC sky images include cloud cover >90%; with sun covered.
- PC sky images include cloud cover between 10% and 90%; sun may or may not be covered by thin or thick clouds.

Figure 3 (Vaucher et al. 2023) provides an example of each sky type as seen in a WSI image.

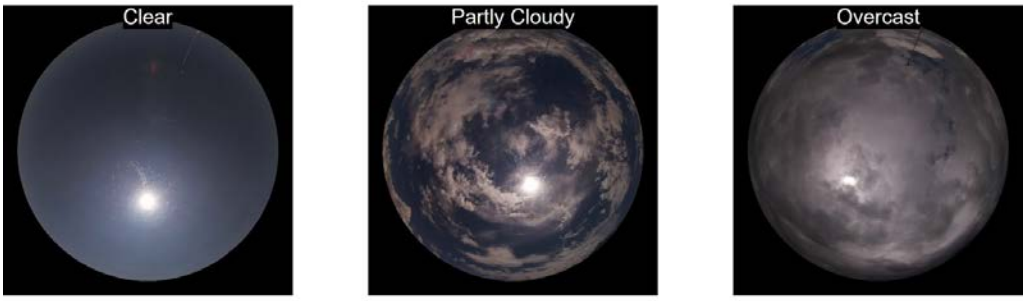

Fig. 3 WSI image examples of CLR, PC, and OVC sky types

After scrutinizing all the sky type cases and experimenting with various analysis tools, it was found that an adjustment to the red frequency recorded in the photo enabled the cloud, sun, and artifact pixels to be isolated from the other WSI features. The near consistent shape of the sun (and a pre-knowledge of its location) enabled its pixels to be distinguished from the other sequestered elements. The solar disc pixel count was compared with that of the entire image, which revealed a correlation with sky types. This process quickly became a significant function of the WSI image analysis routine. (Note: Per Section 1.5.2, the solar disc count included the lens-created corona.) A summary of the other key (Vaucher et al. 2023) study findings follow.

- Under CLR conditions, the geometric shape of the solar disc was closest to a circle (minimal percent sun-corona disc) at its highest point (zenith). The disc became an oval (larger percent magnitudes) as the sun nears the horizon, due to lens distortions. The highest sun position in the sky dome image occurred at approximately 1300 MDT.
- CLR sky conditions generated percent sun disc magnitudes between 0.20% and 0.55%, with an average value of 0.34%, and a minimum/maximum spread of approximately 0.2%.

- OVC sky conditions generated percent magnitudes between 0.00% and 0.26%, with an average value of 0.03%.
- PC sky conditions varied greatly. After removing near OVC, no sun and thick clouds, the minimum/maximum percent sun disc spread was between 0.2% and 0.4%.
- PC conditions were divided into thin and thick cloud types covering the sun disc. The thick cloud occultation produced results that imitated OVC sky conditions. The thin cloud occultation showed a scattered version of almost CLR sky magnitudes.

A tabulated summary of the "sun pixels to sky type" results and their significance is elaborated in Section 3.

3. WSI Image Analysis: Method Advancements

In this section, the method used to quantify the current cloud cover from a WSI image is described. The overarching approach can be summarized in two steps.

Step 1. Isolate clouds from the non-cloud features found in the whole sky image.

Step 2. Calculate the percent cloud cover based on Eq. 1.

$$Cloud\ Footprint = \frac{Total\ cloud\ pixels}{Total\ sky\ pixels} \times 100\% \quad (1)$$

The numerator is the total number of pixels found within the footprint of all clouds on the sky image. The denominator is the total pixel count of the entire circular sky image (not including the black rectangular frame).

The details within the two steps are described in the following, starting with a review and refinement of the current study's goal, an update to the former algorithms, and the development of a "new" technique for determining the percent clouds present in a WSI image.

3.1 Study Goal

To determine surface solar radiation fluxes, knowledge of the cloud cover filtering the transmission of solar irradiance from space to the surface is required. Meteorological Observers are trained to determine sky type, cloud type, and percent cloud cover. Developing an algorithm to automatically do this same task directed the method that follows.

Note that, although meteorological observations can report cloud cover in eighths, this study purposefully opted to focus on quantifying the cloud cover in the equally accepted meteorological standard of tenths. It is also worth noting that, unlike an Aerographer's Mate Third Class (Observer) training, the cloud cover quantities presented as solar radiation model input were taken from a surface observer's perspective (vs. the projection of how an airplane in flight would view the sky, which is a unique application), and it included a 5% resolution (Orvis 1984).

3.2 Algorithm Updates

The approach an observer uses to determine the percent cloud cover from a WSI image is to visually isolate and estimate all (white to black) clouds from non-cloud objects and compare that approximated "space" covered, with respect to the total 10/10 sky dome.

When a WSI image is displayed, the photograph consists of a rectangular array of pixels. Within the rectangle is a non-black circular area that represents the sky dome (Fig. 1). Focusing the algorithm on the sky dome is the first step. Fortunately, the diameter of a WSI image is very consistent, which enables the sky pixels to be extracted from the black frame using a MATLAB *Image Segmenter* function and its circle mask. Pruning the land features from the sky elements can be done through a diameter adjustment.

3.2.1 Solar Disc Algorithm Update

The original percent solar disc determination uses a comparison of the total sun (and corona) pixels derived from using the RGB method of color thresholding versus the total pixels of the acquired rectangular image. Consequently, each whole sky image included a black frame around the circular footprint of sky pixels. Including this frame is a valid approach; however, a more descriptive and flexible approach is to compare the total sun pixels with the total circular sky pixels (Eq. 2).

$$Sun\ Footprint = \frac{Total\ Sun\ pixels}{Total\ sky\ pixels} \times 100\% \quad (2)$$

Referencing the main image analysis program (provided in Appendix B), this denominator correction required an adjustment to the "*FiltersRegions*" function (Fig. 4).

```
function [a, BW2, properties, sun, remainingarea] =filterRegions(BW1)
% function [a, BW2,properties, whitepixs, cloudpixs, sunpixs,CC] = filterRegions(BW1)
%filterRegions Filter BW image using auto-generated code from imageRegionAnalyzer app.

% Auto-generated by imageRegionAnalyzer app on 13-Jul-2022
%-----------------------------------------------------------

BW2 = BW1;

% Get properties.
properties = regionprops(BW2, {'Area', 'Eccentricity', 'EquivDiameter', 'EulerNumber', 'MajorAxisLength', 'MinorAxisLength', 'Orientation', 'Perimeter'});
% determiene the percent of pixels in the image that are nonzero (nonzero =
% white pixels)
a = (nnz(BW2)/numel(BW1))*100;

end
```

Fig. 4 Original *FilterRegions* function using a rectangular image pixel count

The original equation (Fig. 4) instructs the computer to do a different task, namely,

$$a = \left(\frac{nnz(BW2)}{numel(BW1)}\right) * 100\%. \quad (3)$$

In this formula, BW2 represents a binary sun mask, where all pixels of the sun have been converted into a "1" value. The *nnz* argument is the sum of all pixels within that region of interest (ROI). BW1 represents the binary mask of the circle portion of the WSI image. The *numel* argument is the sum of the entire image (the rectangular photo) regardless of the ROI. By changing *numel* to *nnz*, the denominator now represents just the circle portion of sky image

$$a = \left(\frac{nnz(BW2)}{nnz(BW1)}\right) * 100\%. \quad (4)$$

With the denominator value reduced, the threshold ratios for defining sky types by the solar disc had to be adjusted.

3.2.2 New Solar Disc Thresholds for Sky Type Determination

The baseline shift from a rectangular pixel count (1,048,576 pixels) to the circular sky portion of the WSI only (666,999 pixels) created a net increase to the original sun percentage magnitudes, of approximately 36%. We subdivided the results into their sky types, and the 5-day samples representing each category are shown in Figs. 5–12. The original results using a rectangular baseline are displayed first followed by the updated circular sky baseline. As expected, the relative curve shapes were preserved and only the magnitude of the percent sun disc results were changed.

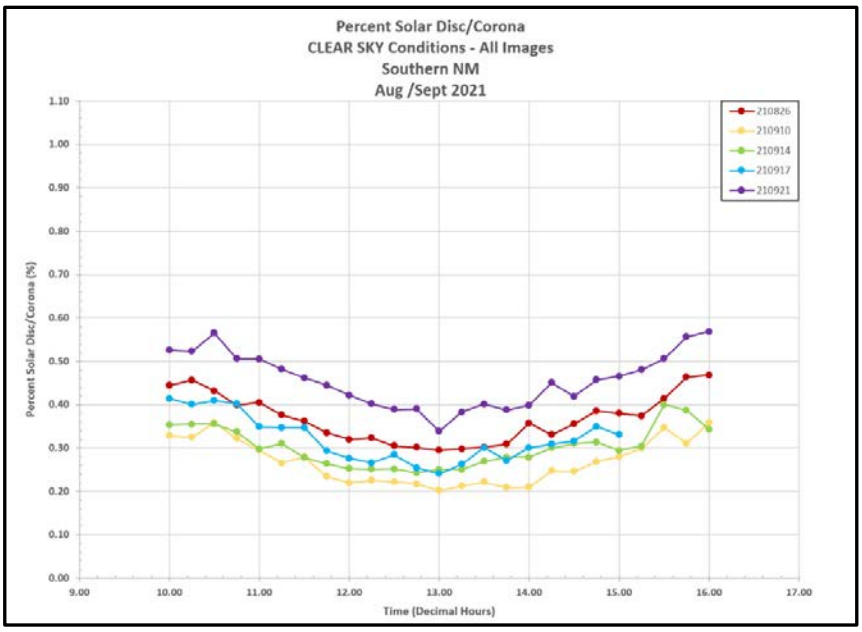

:

Fig. 5 CLR: percent solar disc/corona using a rectangular image baseline

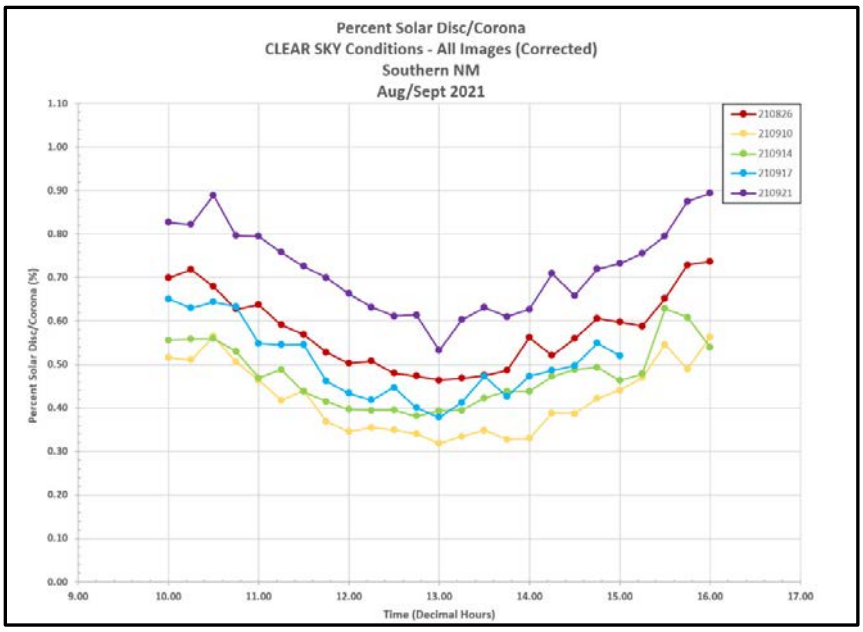

Fig. 6 CLR: percent solar disc/corona using circular sky image baseline

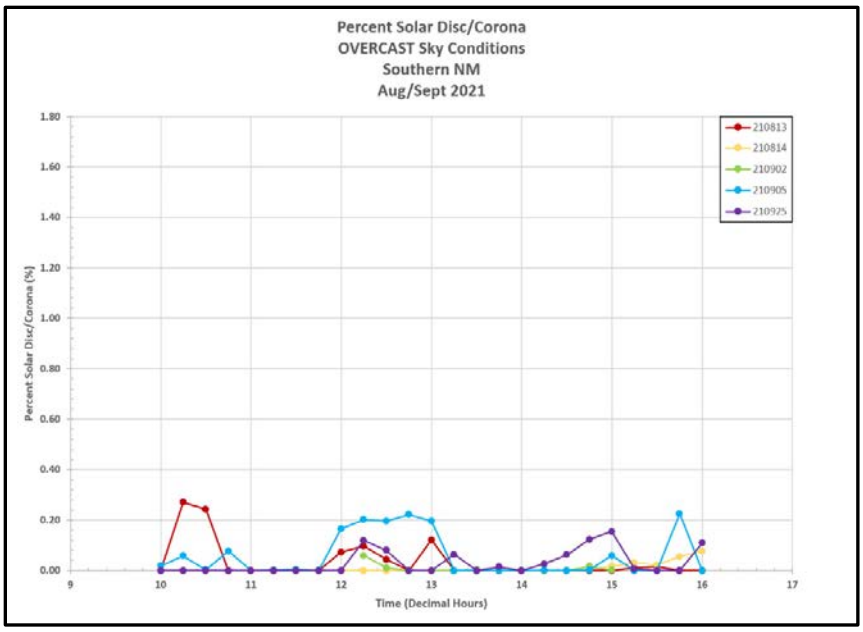

Fig. 7 OVC: percent solar disc/corona using rectangular image baseline

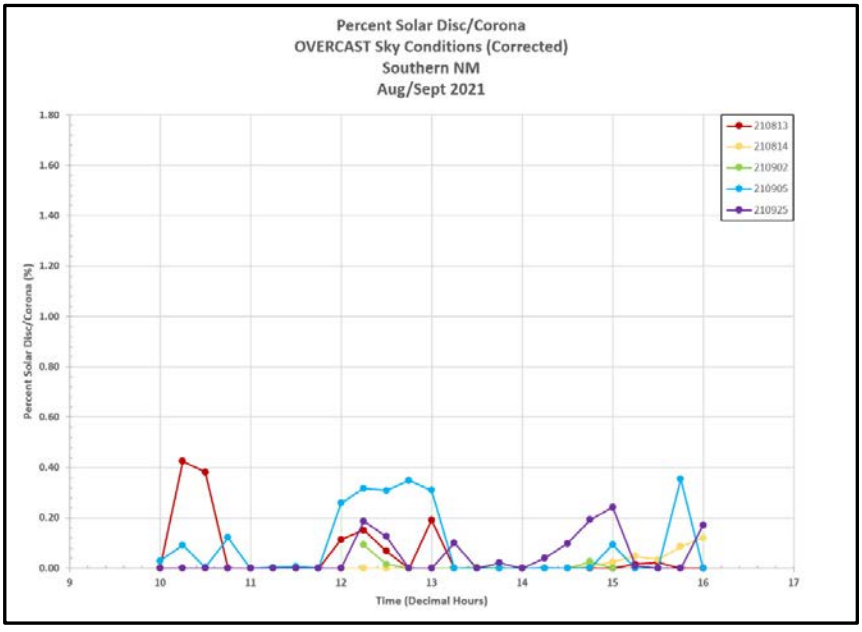

:

Fig. 8 OVC: percent solar disc/corona using circular sky image baseline

The complex nature of the PC cases prompted the rectangular versus circular baseline results to be grouped into two categories. The first category included all PC cases as defined by the amount of cloud cover visually evaluated within the image. That is, each analyzed image had between 10% and 90% clouds showing within the photograph (see Figs. 9 and 10).

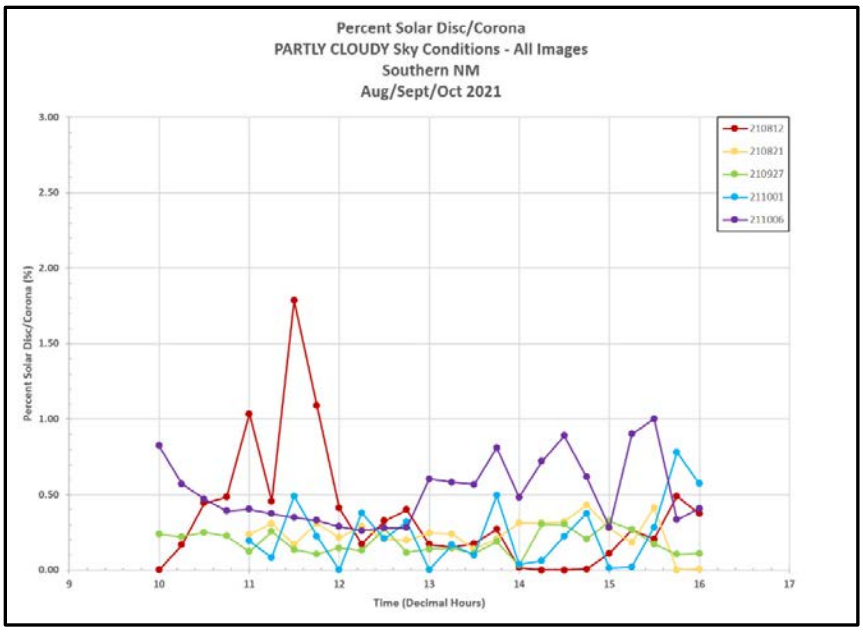

Fig. 9 PC: percent solar disc (all images) using rectangular image baseline

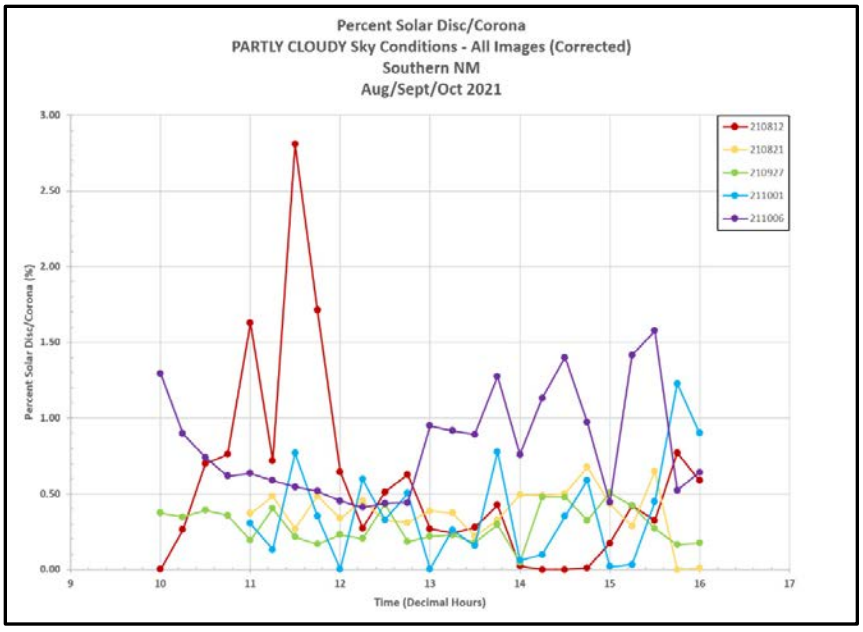

Fig. 10 PC: percent solar disc (all images) using circular sky image baseline

The second PC category continued the train-of-thought initiated in Vaucher et al. (2023). When the sun was not observed or the thickness of the cloud closely imitated OVC conditions, these cases were removed from the PC evaluation. The net result was the removal of 20 images or approximately 19% of the PC cases (see Figs. 11 and 12).

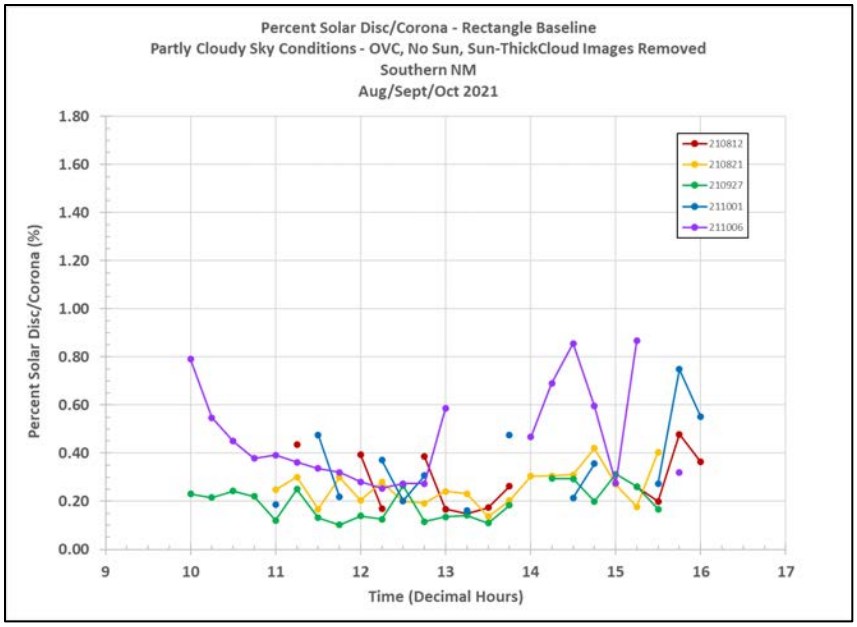

Fig. 11 PC: percent solar disc (filtered images) using rectangular baseline

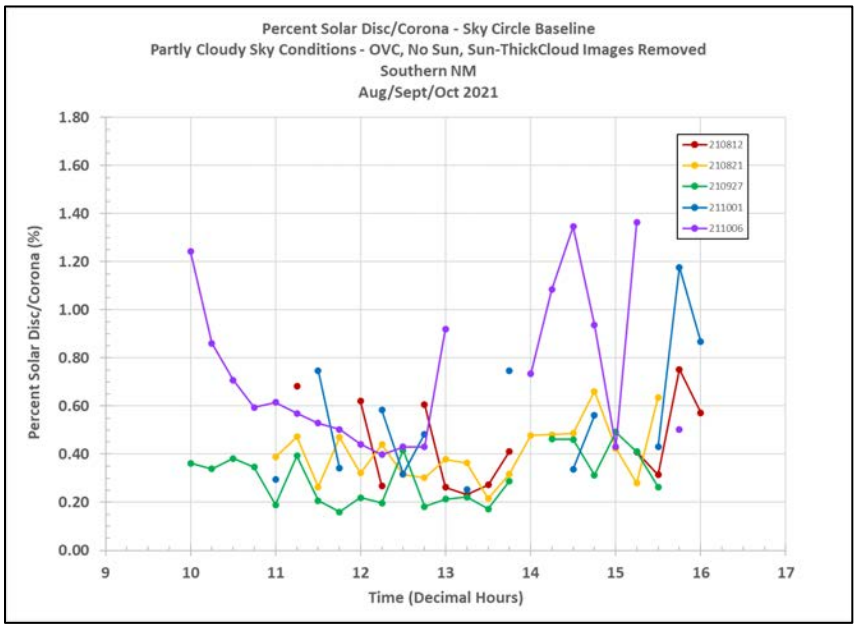

Fig. 12 PC: percent solar disc (filtered images) using circular sky baseline

Tables 3 and 4 describe both baseline approaches statistically. Figure 13 aligns the solar disc thresholds by their sky condition, using rectangular and circular baselines, respectively.

Table 3 Percent sun pixels (rectangular baseline) vs. sky type

Rectangle base cases: sky type validated data	Number of cases	Min (%)	Max (%)	Avg (%)	Std (±)
CLR	121	0.20	0.55	0.34	0.05
OVC	108	0.00	0.26	0.03	0.05
PC – No sun and/or thick clouds were removed	86	0.10	0.87	0.31	0.13
PC – All variations of PC included	106	0.002	1.71	0.33	0.20

Table 4 Percent sun pixels (circular baseline) vs. sky type

Circle sky base cases: sky type validated data	Number of cases	Min (%)	Max (%)	Avg (%)	Std (±)
CLR	121	0.31	0.87	0.53	0.05
OVC	108	0.00	0.41	0.05	0.08
PC – No sun and/or thick clouds were removed	86	0.16	1.36	0.48	0.20
PC – All variations of PC included	106	0.002	2.69	0.52	0.31

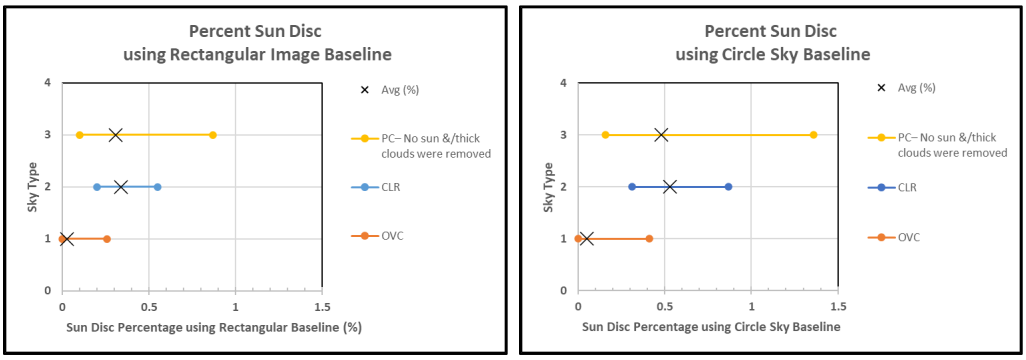

Fig. 13 PC, CLR, and OVC percent sun using rectangular (left panel) and circle baselines (right panel)

The results from these cases unfortunately provided no sharp dividing line that would fully distinguish OVC from CLR conditions for either baseline approach. However, the trend and tendency for each sky type were strong enough that, coupled with additional information, a path forward was possible. For example, the OVC solar disc did not exceed 0.41%, nor did the minimum CLR go lower than 0.31%. This would imply that an analyst could use a solar disc size of a "less than 0.31%" threshold to label the conditions as OVC, pending a second approach to validate the status.

Extending this reasoning to PC cases in which the "no sun and thick cloud samples" were removed, this OVC solar disc threshold might have to be lowered to 0.16%. The clear message was that this approach has potential when coupled with additional sky type validation methods. Fortunately, another informative method was found that focused not on the cloud cover, but instead on the distribution of

blue sky (see Section 3.4). In the meantime, the next issue we addressed was the separation of non-cloud objects from the RGB cloud pixel count.

3.3 Quantifying Non-cloud Objects

We used the RGB approach to isolate cloud cover and found that artifacts, fixed ground objects, and lens flares were often included in the "cloud" pixel count. Consequently, we pursued a quest to isolate and remove these objects. The following demonstrates the extraction of pixels representing the stationary Meteorological Measurement Tripod (MMT) that was sampling data near the WSI.

The CLR sky case of 2021 September 9, 1300 MDT was selected to isolate the artifacts, fixed ground objects, and lens flare from cloud pixels (Fig. 14). The theory was that under clear skies, no clouds would be present, and all pixel counts would represent objects needing to be extracted from the cloud pixel tally.

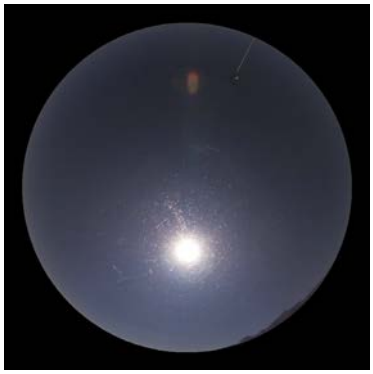

Fig. 14 CLR case: 2021 September 9, 1300 MDT

The image was processed using an RGB image analysis technique. As expected, all non-blue sky objects highlighted were not clouds but visible items. As Fig. 15 shows, these included the MMT (a ~1-cm-long line in the upper right corner), a sun or lens flare (teardrop shape with a red hue), the sun with its rough-edged corona (a quasi-circular object), and a thin strip of distant mountains on the sky horizon (lower right corner).

Fig. 15 CLR case: function highlights non-blue sky features

The area around the MMT object was isolated and converted to a grayscale, and pixels greater than "0" were used to create a white mask of the object (to verify the targeted object). Once verified, an inverse function converted the object into 0 values. This mask was returned to the main program for integration into the original photo. Figure 16 shows a close up of the original and postprocessing image of the MMT, with black colored objects assigned 0 magnitudes.

Fig. 16 CLR: function isolated or removed fixed ground object (MMT)

After converting the mask into an unsigned 8-bit integer value, we were able to assess how many pixels this object consumed with respect to the circular sky footprint. (Note that similar to the cloud pixel count spillage, the isolation of the object had to be refined significantly, to avoid the inclusion of surrounding non-tripod objects.)

Returning to the original full image, the refined tripod mask was applied to the image, with the results as seen in Fig. 17. The mask is seen as a black (0 valued) silhouette-like object in the upper right corner of Fig. 17. Note that the images were brightened by 36 units in this publication, to better view the distinction of photographic features.

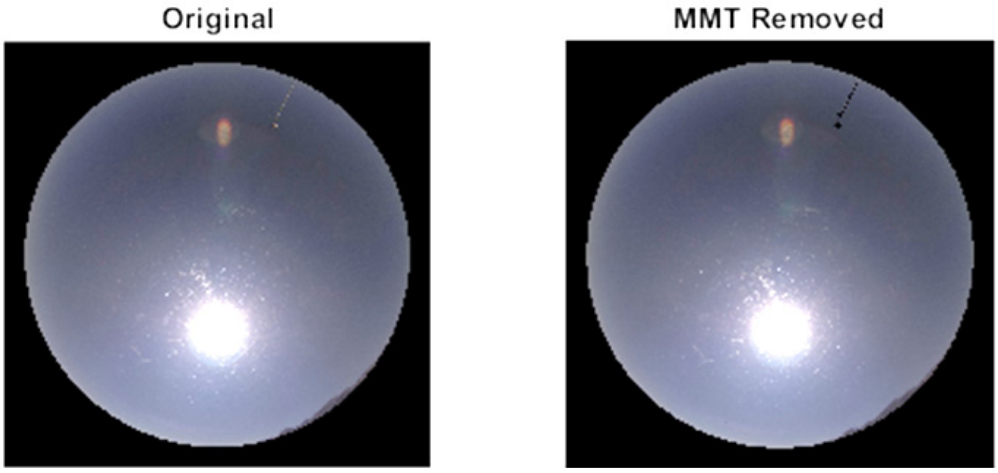

Fig. 17 CLR: MMT mask applied to original image (upper right corner)

As a final step, an analysis of the object mask for the MMT was conducted to determine what percentage of the total pixel count this represented. The assessment included a cross-check of results from other WSI images. The total tripod pixel count was approximately 500–530 pixels, or 0.07%–0.08% of the total circular WSI image.

Extending this analysis to the other two major objects, that is lens flare and sun disc, the results show their pixel footprint to be 0.44% and 0.52% of the total sky image, respectively. These findings mean that the entire pixel representation by the non-sky and non-cloud objects comprise less than 1.1% of the total sky pixel count.

Table 5 gives an example of the pixel distribution for the CLR, 2021 September 21, 1300 MDT case. Note that coupling the sun and corona pixels in this case resulted in a corona/sky pixel count overlap with the sky pixels, of approximately 0.3% (0.25%), which was recognized and removed to balance the tally.

Table 5 Percent pixel tally for CLR case: 2021 September 21, 1300 MDT

CLR: 2021 September 21, 1300 MDT WSI objects	**Percent pixels** Total circular sky pixels
Sky	97.51
Sun and corona[a]	2.01
Lens flare	0.44
Meteorological tripod	0.07
Total %pixels	100

[a] 0.25% overlapping sky/sun corona pixels removed

Translating this balanced concept into a more formal equation, the total sky pixels would be the sum of its component pixels:

$$Total\ WSI\ Sky\ Pixels = Clouds + Blue\ Sky + Lens\ Artifacts + Physical\ Objects \quad (5)$$

If the total WSI sky pixels is fixed, the artifacts and physical objects represent less than 3% of the total sky. Assimilating this perspective, the primary focus of the WSI image analysis rests on cloud and blue sky pixel counts. The cloud pixel count was already determined to be inexact yet promising. In the next Section 3.4, the remaining factor is investigated; namely, blue sky pixels.

3.4 Image Analysis: Quantifying Clouds as Function of Blue Sky

Validating a solution is typically done by independently attaining the results and cross-checking the solution. For the cloud assessment, this strategy was implemented by having trained meteorologists separately execute sky and cloud evaluations.

It was not practical to automate such a cloud validation process (human evaluations). Thus, another approach was pursued; namely, to run the problem backwards. Using Eq. 5, the total pixel count for a sky baseline was known. Cloud pixel counts with the up to 3% spillage pixels for artifacts and other local objects could be approximated. The missing component was determining the non-cloud pixel count, which is also known as the blue sky pixels count.

3.4.1 Blue Sky Algorithm

The most effective function for capturing the blue sky regions of the WSI was the HSV color model. Quantifying the blue sky pixels followed the pattern of Eq. 6, where

$$Percent\ Blue\ Sky = \frac{Total\ BlueSky\ Pixels}{Total\ WSI\ Sky\ Pixels} \times 100\%. \quad (6)$$

To demonstrate the algorithm, the PC sample from 2021 October 1, 1300 MDT is used (see Fig. 18). The independently estimated cloud cover for this image was between 50% and 60% (recommending a 55% data entry).

Fig. 18 PC sky sampled from 2021 October 1, 1300 MDT

A binary mask for the blue pixels was created using the *Color Thresholder* application. With the WSI image selected, the HSV color model was chosen. The hue values were given a new shade of color range, namely, 50–70 units. The saturation and value were left at their default "pure color" and "overall brightness" quantities. Figure 19 shows the results for these parameter selections. Note that the non-blue-sky regions were assigned a 0 value. Having 0 value, they appear black to the viewer.

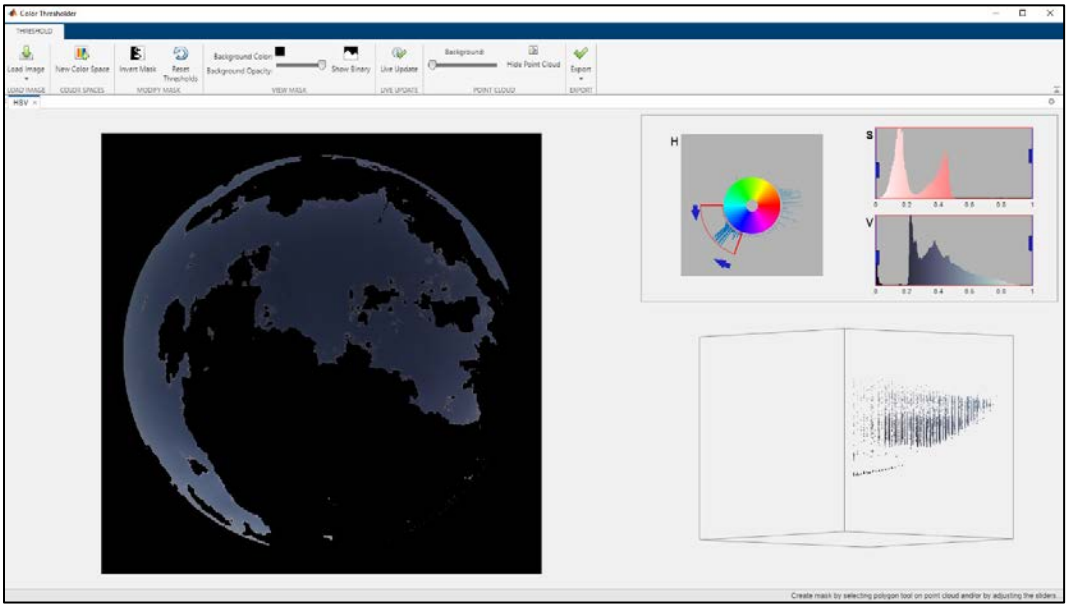

Fig. 19 PC: 2021 October 1, 1300 MDT; H (50–70 units), S (default), and V (default)

The image was then converted into a binary format. Selecting “Show Binary” converts all non-black pixels into white pixels (1s). When excess pixels were noted outside the ROI (Fig. 20, rectangular frame area), the overall brightness “V” range was reduced from (0 ➔ 1) to (0.1 ➔ 1.0) Figure 20 shows the net outcome of the image transformation into black and white pixels.

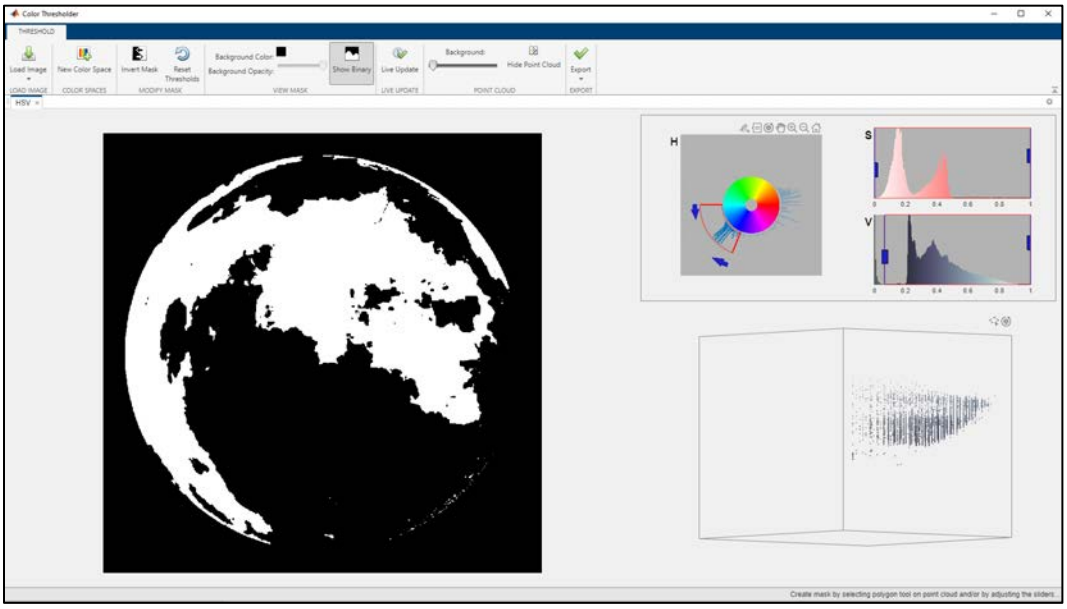

Fig. 20 PC: 2021 October 1, 1300 MDT; binary blue sky area shown in white (1s)

The results were then exported and given a binary mask name (such as BW_BlueSky). The *Image Region Analyzer* application tabulated the white pixel totals for the blue sky mask, where white = 1. Using the command line equation of

$$BlueSky\_Total = nnz(BW\_BlueSky), \tag{7}$$

the total blue sky count was reported as 294,573 pixels. Comparing this value to the sky image total (666,999 pixels), the percentage of blue sky was calculated to be 44.16%. Making a presumption that what is not blue sky is cloud, one can subtract this value from 100%, leaving 55.83% (56%) of the image as showing cloud cover, which is between 50% and 60%, close to the recommended data entry value (55%).

For coding purposes, the final step of the process can be reduced to the following equation:

$$Percent\ Cloud\ Cover = \left[1 - \left(\frac{nnz(BW\_BlueSky)}{nnz(Total\ Sky\ Pixels)}\right)\right] \times 100\%. \tag{8}$$

3.4.2 Significance of Blue Sky Approach

Earlier, the sun disc percent was found to be imperfectly correlated with the sky type. An independent quantification check was recommended, so the net result could determine the sky type and, ultimately, a useful cloud cover assessment for the solar radiation model input. By knowing the blue sky percentage, its inverse value determined the cloud cover. In other words, to determine sky type, cloud cover needs to fall within the standard guidance of the following.

- CLR sky images include cloud cover <10%; with the sun not covered.
- OVC sky images include cloud cover >90%; with sun covered.
- PC sky images include cloud cover between 10% and 90%; sun may or may not be covered by thin or thick clouds.

When seeking sky type as a function of blue sky, these thresholds are reversed.

- CLR sky images include blue sky values of >90%; with the sun not covered.
- OVC sky images include blue sky values <10%; with the sun covered.
- PC sky images include cloud cover between 10% and 90%; sun may or may not be covered by thin or thick clouds.

Assimilating the cloud cover and blue sky algorithm results significantly enhances the potential for both determining and validating (within a reasonable percent error) cloud cover from a digital WSI image.

4. Application and Results

The improved techniques described above were applied to the 15 WSI images representing clear (5), overcast (5), and partly cloudy (5) sky conditions. Appendix C shows the RGB and HSV results for each case. The quantitative results were examined for two end results: 1) a validation of the calculated percent cloud cover and 2) a calibration of the total image analysis pixel counts.

4.1 Percent Cloud Cover Validation

Each of the 15 WSI image cases were independently examined by a meteorologist or sky observer who provided a percent cloud cover for each photo. Unlike normal observations, the percent cloud cover was taken from the perspective of solar radiation reaching the surface. The observer was also allowed to advise on “half” values. For example, if the percentage fell between 30% and 40%, the selected value for this research task could be listed as 35%.

The calculated percent cloud cover was determined by first computing the difference between the total WSI pixel count and the blue sky mask pixel count. Then, a percentage was calculated with respect to the circular total pixel count of the WSI. Table 6 displays the results of the observed and calculated cloud covers for each of the 15 cases.

Table 6 Observed vs. calculated cloud cover for 15 cases and 3 sky types

WSI Date	WSI Time	OBSERVED Cloud Cover	CALCULATED Cloud Cover
YYMMDD (MDT)	hhmm (MDT)	Percent	Percent
OVC	OVC	OVC	OVC
210813	1300	90	90.1
210814	1300	100	97.1
210902	1300	90	89.2
210905	1300	80-90 (85)	82.4
210925	1300	100	99.4
CLR	CLR	CLR	CLR
210826	1300	0	1.9
210910	1300	0	0.8
210914	1300	0	1.2
210917	1300	0	1.9
210921	1300	0	2.5
PC	PC	PC	PC
210812	1300	25	25.9
210821	1300	25	27.7
210927	1300	30-40 (35)	36.3
211001	1300	50-60 (55)	55.8
211006	1300	25	23.4

The OVC cases showed good agreement, with the 2021 September 5 case having the widest variability. This September WSI image was a marginal OVC case, leaning more toward the PC category. Consequently, it was not surprising to see the results confirming this borderline scenario.

The CLR cases were all within a 3% difference, re-enforcing the ongoing challenges in interpreting the 1) solar disc size, 2) sun corona and lens artifacts appearing like clouds, and 3) horizon “noise” (mountain profiles). Having defined the CLR limitations to be within 3%, these results were considered acceptable.

The PC cases produced favorable results. The scattered and sometimes broken cloud distributions in the images presented a complexity for even the observer. Taking advantage of the mid-point selection option, however, an affirming match is seen between the observers’ selection and the calculated method.

4.2 Calibration of WSI Pixel Analysis

This study investigated all the major elements within the WSI images. These features have been identified and quantified using various RGB and HSV techniques. To determine the effectiveness of these methods, a tally of the image elements was conducted, presuming that the summed pixels analyzed would equal the total WSI image pixel count. If the pixel count came up short, then another WSI element would need to be pursued. If the pixel count exceeded the total, a duplication of counts would be present in the current techniques. If this surplus was of significant magnitude, the techniques would need to be revisited.

Table 7 displays the net results from the 15 cases (3 sky types). The percent values were derived from the pixel counts using the round WSI as the total pixel count. The three major image elements tallied for the count included the solar disc (sun), the blue sky, and the MMT. The Mask for each component was determined independently. To calibrate the results, the total pixel count for the WSI image was considered a fixed value. For this calibrating analysis, only the sun, blue sky and cloud cover were included in the summation.

Table 7 Standard (Std) vs. calculated (Calc) WSI sky totals

Date	Local Time	Total WSI	Sun	Blue Sky	MMT	Calc Cloud Cover	Std Total Sky	Calculated Total Sky (no MMT)	Total Sky Difference (Calc - Std)
YYMMDD	Hrs	Pixels	Percent	Percent	Percent	Percent	Percent	Percent	Percent
								OVC=(S+B+C)	
210813	1300	666999	0.1909	9.8964	0.1840	90.1036	100.0	100.1909	**0.1909**
210814	1300	666999	0.0000	2.9297	0.0865	97.0703	100.0	100.0000	**0.0000**
210902	1300	666999	0.0000	10.7633	0.2894	89.2367	100.0	100.0000	**0.0000**
210905	1300	666999	0.3096	17.5658	0.0942	82.4342	100.0	100.3096	**0.3096**
210925	1300	666999	0.0000	0.6492	0.0820	99.3508	100.0	100.0000	**0.0000**
								CLR=(S+B+C)	
210826	1300	666999	0.4637	98.0637	1.8604	1.9363	100.0	100.4637	**0.4637**
210910	1300	666999	0.3183	99.1745	1.8499	0.8255	100.0	100.3183	**0.3183**
210914	1300	666999	0.3937	98.7538	1.8244	1.2462	100.0	100.3937	**0.3937**
210917	1300	666999	0.3789	98.0813	1.8622	1.9187	100.0	100.3789	**0.3789**
210921	1300	666999	0.5322	97.5288	1.8690	2.4712	100.0	100.5322	**0.5322**
								PC=(S+B+C)	
210812	1300	666999	0.2684	74.1307	1.7664	25.8693	100.0	100.2684	**0.2684**
210821	1300	666999	0.3855	72.3054	1.9249	27.6946	100.0	100.3855	**0.3855**
210927	1300	666999	0.2181	63.6731	1.4220	36.3269	100.0	100.2181	**0.2181**
211001	1300	666999	0.0030	44.1639	1.2313	55.8361	100.0	100.0030	**0.0030**
211006	1300	666999	0.9486	76.6078	1.7978	23.3922	100.0	100.9486	**0.9486**

As seen in Table 7, the OVC cases showed that 60% of the results matched the total pixel count. The cases that reported an overlapping pixel count showed a less than 0.3% duplication. The CLR cases showed a consistent trend of overlapping pixel counts, between 0.3% and 0.5%. The PC case results ranged between 0 and 0.9%. Putting these findings in context, all of the results were less than the previously

accepted 3% buffer for lens artifacts and other stationary elements. For calculating solar radiation, these outcomes are well within acceptable levels.[†]

5. Summary and Conclusions

The need to interpret WSI images stems from an input requirement of a surface solar radiation flux model supporting the forecast of PV power generation. Foundational research defined an algorithm that determines the sky type based on the solar disc size, using an RGB thresholding method. The nonlinear correlations between sky type and solar disc size led to the pursuit of a second image analysis method to refine the initial mixed results.

Beginning with a review of the professional (human) cloud cover quantification techniques, we discovered a subsequent procedure using HSV to highlight the blue sky pixels of the WSI. This effective method was successfully applied to masking the individual non-moving ground objects as well. A MMT masking algorithm was added to the WSI analysis.

The blue sky algorithm we developed was used to calculate the cloud cover by interpreting all non-blue sky pixels as clouds. Having determined that the sun's corona and image artifact features represented less than 3% of the total pixel count, the calculated cloud cover was compared to the meteorologist or sky observer values.

- Cloud cover for OVC cases showed good agreement between the observer and calculated values. The largest calculated-observed difference was from a borderline OVC/PC image.
- The no cloud cover of CLR cases were all within a 3% difference, reinforcing the ongoing challenges in interpreting the solar disc size, the sun corona and lens artifacts appearing like clouds, and horizon noise (profiles of towers, mountain, etc.).
- The PC cloud cover cases produced favorable results with the inclusion of mid-point selection options for the observer's assessment.

To better assess the masking technique, a tally of all WSI image elements was cross-checked against a full WSI pixel quantification. Using the same 15 cases

[†] Note: Appendix C shows the tallies, which include the MMT element as well. In some cases, the MMT element was part of the other elements already reported. Thus, for the standard analyses, the MMT was not included. With the addition of the MMT component, the net results increased by ~3%.

(three sky types), the sum totals of sun, blue sky, and cloud cover were compared to the total possible WSI (circle) pixels.

The results showed that for the OVC cases, 60% of the results matched the total pixel count. A total pixel excess of no more than 0.3% was reported in the balance of cases. The CLR cases showed a consistent trend of overlapping pixel counts, between 0.3% and 0.5%. The PC case results ranged between 0 (perfect match) and 0.9% (pixel duplication).

Based on the ease in picking up stray pixels when masking, the results were well within the accepted buffer for representing lens artifacts, ground silhouettes, and others. For calculating solar radiation, these findings were well within acceptable levels.

In conclusion, the research we conducted has improved WSI image analysis capabilities by accounting for all the major elements within the WSI images. The algorithms developed are poised for their application in preparing data for the solar radiation model input. As the process becomes more precise and accurate, the ability to integrate solar fuels into the hybridized tactical and civilian power resources will improve, thus reducing Warfighter vulnerabilities to enemy forces and delayed recoveries in disaster relief emergencies.

6. References

American Meteorological Society. Cloud classification. Glossary of meteorology; n.d. [accessed 2022 Aug 12]. https://glossary.ametsoc.org/wiki/cloud_classification.

Image Engineering. Image quality factors white balance; c2022 [accessed 2022 Aug 12]. https://www.image-engineering.de/library/image-quality/factors/1079-white-balance.

National Weather Service. Cloud classification. US Department of Commerce, National Weather Service, National Oceanic and Atmospheric Administration (US); 2020 May 30. https://www.weather.gov/lmk/cloud_classification.

Orvis WA. Aerographer's mate third class (observer). Naval Education and Training Command, Department of the Navy (US); 1984. NAVEDTRA 101570.

SSERC. Measuring cloud cover. Scottish Schools Education Research Centre (SSERC); c2021 [accessed 2024 May 31]. https://www.sserc.org.uk.

The GLOBE Program. Measuring cloud cover. The GLOBE Program, Global Learning and Observations to Benefit the Environment; n.d. [accessed 2024 May 31]. https://www.globe.gov/web/s-cool/home/observation-and-reporting/obser1ving-cloud-cover.

The MathWorks, Inc. Understanding color spaces and color space conversion; c2024 [accessed 2024 May 31]. https://www.mathworks.com/help/images/understanding-color-spaces-and-color-space-conversion.html.

Vaucher G, D'Arcy S, Berman M. In-situ atmospheric intelligence for hybrid power grids: volume 1 (feasibility study). Army Research Laboratory (US); 2019 Dec. Report No.: ARL-TR-8864.

Vaucher G, Goodman H, Wang B, Lee M. Atmospheric intelligence for hybrid power advancements: volume 2 (whole sky image percent cloud and sun analyses). DEVCOM Army Research Laboratory (US); 2023 May. Report No.: ARL-TR-9682.

Vaucher G, Jane R, Whitaker, J. In-situ atmospheric intelligence for hybrid power grids: volume 5 (ambient versus panel temperature for PV power models). DEVCOM Army Research Laboratory (US); 2022 May. Report No.: ARL-TR-9454.

Vaucher G, Lee MS, Goodman H. In-situ atmospheric intelligence for hybrid power grids: volume 3 (analysis of whole sky image compression). DEVCOM Army Research Laboratory (US); 2021 Dec. Report No.: ARL-TR-9360.

Weldon RL. Quartermaster 3. Department of the Navy (US); 1985. NAVEDTRA 10157.

Appendix A. Whole Sky Imager Test Images by Sky Type and Special Cases

Appendix A is a courtesy reprint of ARL-TR-9682, Appendix A.[1] It contains examples of the whole sky image data used in this report's research analyses. These data files were acquired over Southwestern, New Mexico, at a location called "Site B." The displayed images were taken at 1300 MDT and provide a midday sunlight snapshot of the five clear ([CLR] Fig. A-1), five overcast ([OVC] Fig. A-2), and five partly cloudy ([PC] Fig. A-3) cases discussed in the technical report. Two sequenced special case images (Fig. A-4) show a 22° halo as part of the 2021 September 25 OVC case at Site B.

Photos are aligned so that north is up and east is to the left. The diurnal solar path traverses the image from left (east) to right (west). Date labels/captions for each image are in a two-digit year, month, day (YYMMDD) format. For additional information, see Section 1.2 and Table 1 of the main report.[1]

[1] Vaucher G, Goodman H, Wang B, Lee M. Atmospheric intelligence for hybrid power advancements: volume 2 (whole sky image percent cloud and sun analyses). DEVCOM Army Research Laboratory (US); 2023 May. Report No.: ARL-TR-9682.

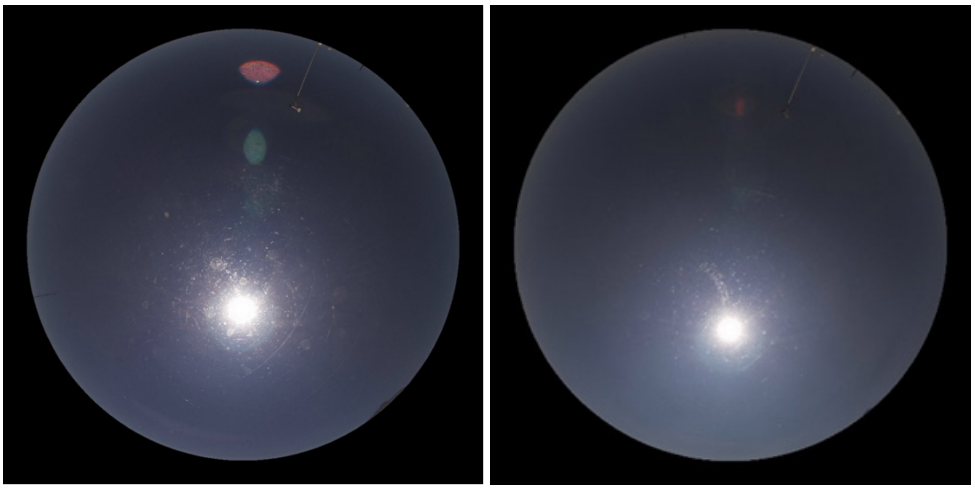

(a) 210826, 1300 MDT (b) 210910, 1300 MDT

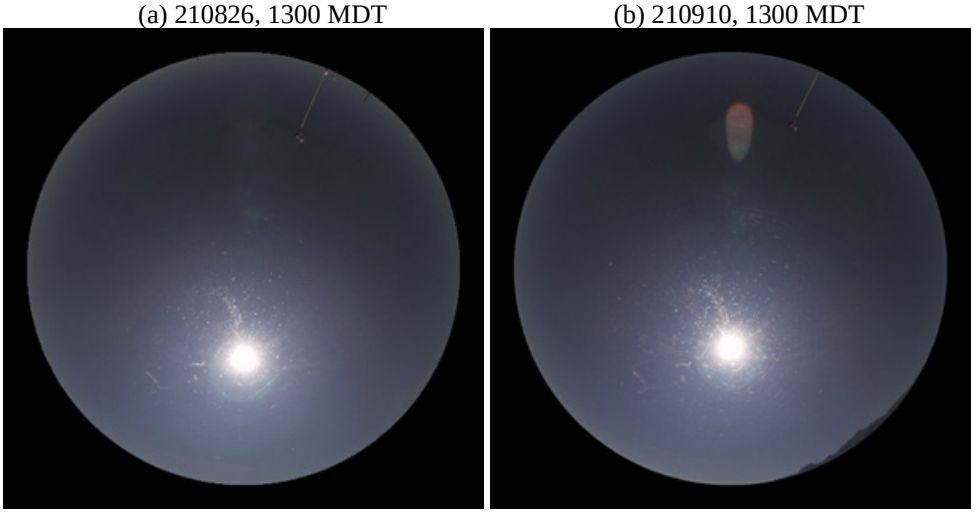

(c) 210914, 1300 MDT (d) 210917, 1300 MDT

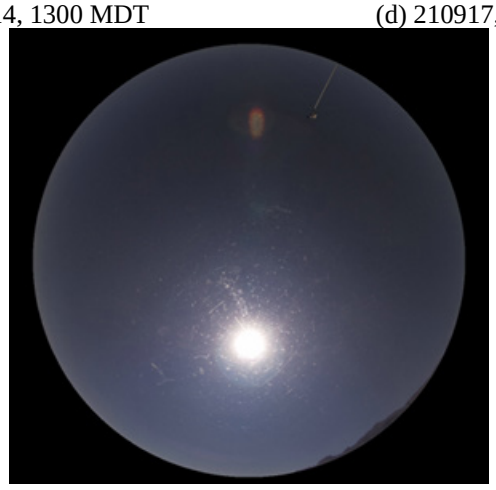

(e) 210921, 1300 MDT

Fig. A-1 Five CLR cases: Site B[2]

[2] Vaucher G, Lee MS, Goodman H. In-situ atmospheric intelligence for hybrid power grids: volume 3 (analysis of whole sky image compression). DEVCOM Army Research Laboratory (US); 2021 Dec. Report No.: ARL-TR-9360.

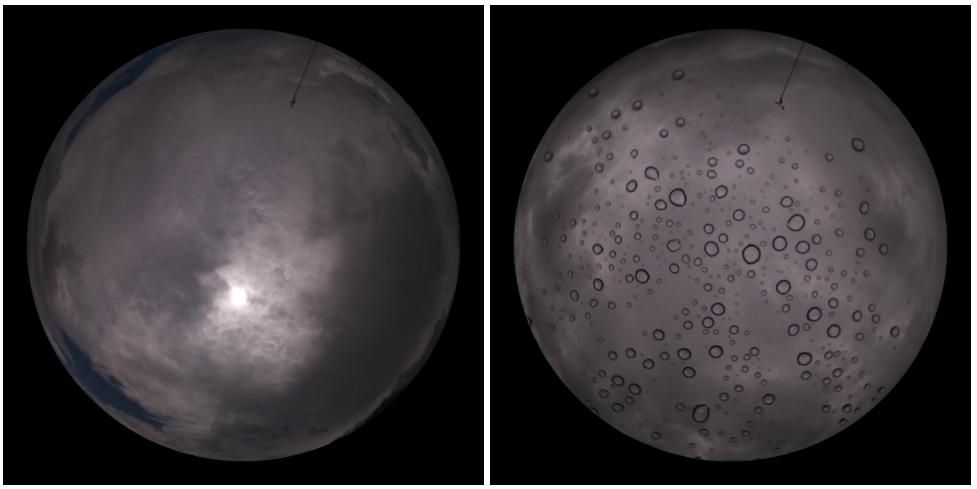

(a) 210813, 1300 MDT (b) 210814, 1300 MDT

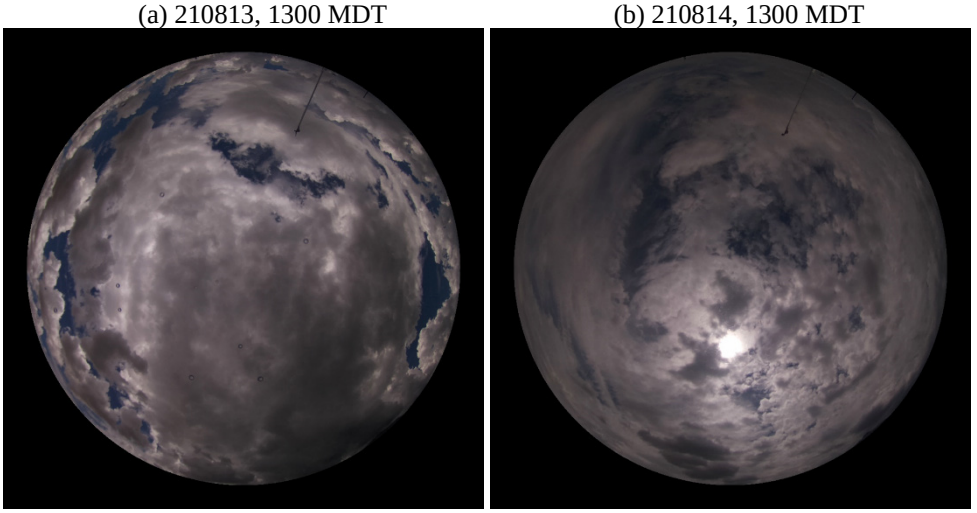

(c) 210902, 1300 MDT (d) 210905, 1300 MDT

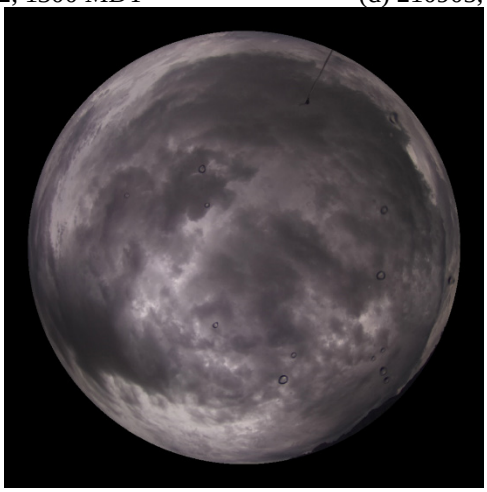

(e) 210925, 1300 MDT

Fig. A-2 Five OVC cases: Site B[2]

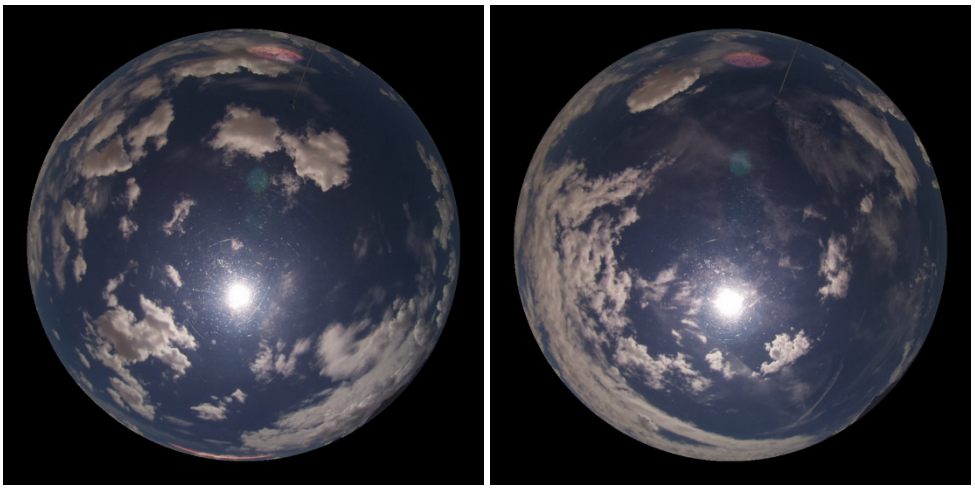

(a) 210812, 1300 MDT (b) 210821, 1300 MDT

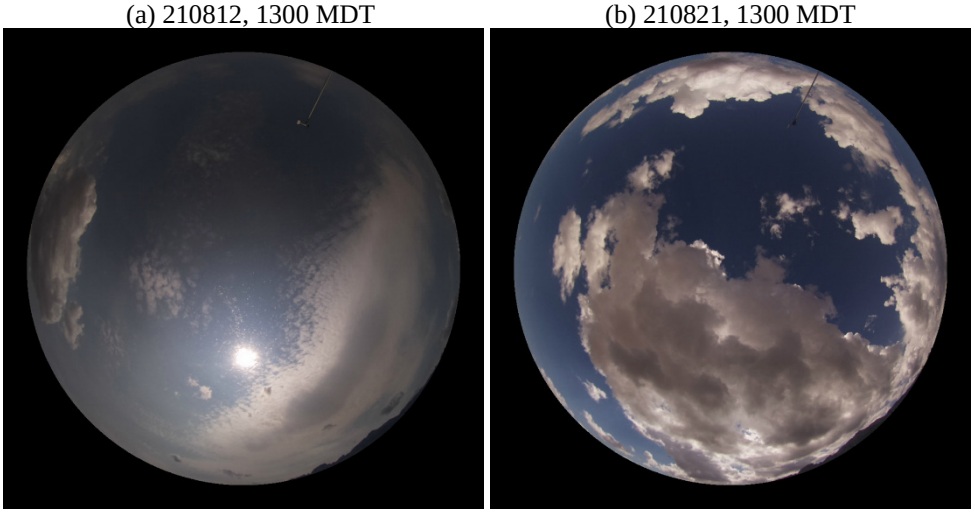

(c) 210927, 1300 MDT (d) 211001, 1300 MDT

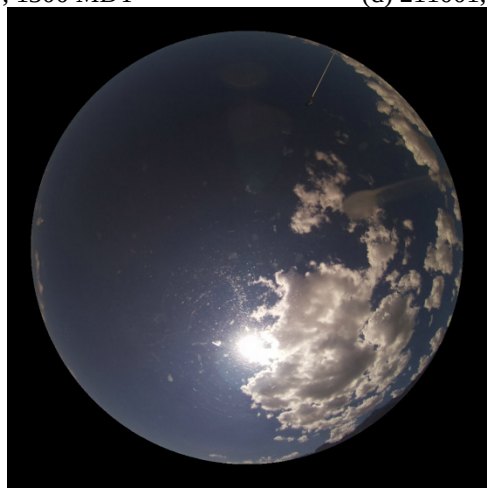

(e) 211006, 1300 MDT

Fig. A-3 Five PC cases: Site B[2]

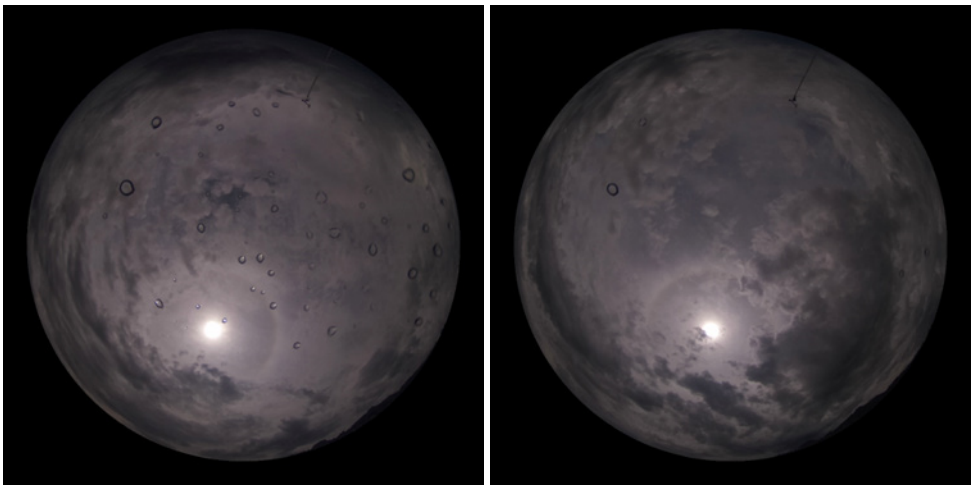

(a) 210925, 1215 MDT (b) 210925, 1230 MDT

Fig. A-4 Two OVC special cases: 22° halo over Site B[2]

Appendix B. Percent Cloud Cover Function

The Percent Cloud Cover algorithm[1] is shown in Fig. B-1. This function uses a ratio of cloud cover pixels to total pixel count to determine the percent cloud cover. The program's update was applied to the *filterRegions* function (Fig. 4) referenced within this code.

[1] Vaucher G, Goodman H, Wang B, Lee M. Atmospheric intelligence for hybrid power advancements: volume 2 (whole sky image percent cloud and sun analyses). DEVCOM Army Research Laboratory (US); 2023 May. Report No.: ARL-TR-9682.

```
% Sun disc test:
clc;
clear;

area = 3.14*460.005^2;

imagefiles = dir('*.jpg');
%to give number of images found
nfiles = length(imagefiles);

for ii = 1:nfiles
    currentfilename = imagefiles(ii).name;
    currentimage = imread(currentfilename);
    images{ii} = currentimage;

    %Can be removed: but displays change in sun location over the time
    %period
    %imshow(currentimage,[]);

    %apply image segmentation
    BW = segmentImage(currentimage);
    %apply RGB color masking for sun
    BW1 = createMask(currentimage);
    %apply image region analysis
    sun = filterRegions(BW1);
%   disp(sun);

    %Test sun foot print for appropriate threshold
    if sun <= 0.3 && sun >= 0
        fprintf('Your sky is overcast\n');
        %now that we know the sky is overcast we can test for cloud layers:
        %Apply RGB color masking for bottom layer
        BWA = findbottomlayer(currentimage);
        %apply image region analysis
        bot = filterRegions(BWA);
        % present bottom layer percent
        disp(bot);
        %Apply RGB color masking for top layer
        BWB = findtoplayer(currentimage);
        %apply image region analysis
        top = filterRegions(BWB);
        % present top layer percent
        disp(top)
        %total CC
        cloudcover = top + bot;
        %Remaining space in WSI circle
        blue = 100 - cloudcover;
        disp(cloudcover);

    elseif sun >= 0.33 && sun <= 0.55
        fprintf('Your sky is clear\n');
        %Clear: does not need to test for specific cloud layers
        fprintf('There is no cloud cover to report\n');
        bot = 0;
        top = 0;
        blue = 100;
    else
        fprintf('Your sky is partly cloudy\n');
        %Partly cloudy: test for cloud layers using specifc thresholds
        %apply image segmentation
        BW = segmentImage(currentimage);
        %apply RGB color masking for sun
        PC = partlycloudyMask(currentimage);
        %apply image region analysis
        cloudcover = filterRegions(PC);
        top = 0;
        bot = 0;
        blue = 100-cloudcover;
        disp(cloudcover)
    end

end
```

Fig. B-1 Percent cloud cover algorithm

Appendix C. Results of RGB and HSV Method Applications

Results from applying the red, green, and blue (RGB) and hue, saturation, and value (HSV) image analysis techniques to the 15 Whole Sky Imager (WSI) images shown in Appendix A follows. The cases represent clear ([CLR] five), overcast ([OVC] five), and partly cloudy ([PC] five) sky conditions. An example of results for each sky type is presented, followed by the cumulative five cases per sky type. Finally, tabulated results are shown that supplement the main report's 1) validation of the calculated percent cloud cover and 2) calibration of the total image analysis pixel counts.

C.1 RGB and HSV Results: Sample Cases by Sky Type

The OVC example selected is from 2021 September 25, 1300 local time (LT). The original image is in the upper right side of Fig. C-1. The image mask (upper left) represents just the WSI image area, which was extracted for this analysis. The RGB sun mask (lower left) shows no data (black pixels have 0 value), because the sun is occulted by the clouds. The HSV image reports hints of the ground landscape in white and very few (<0.7% of WSI image) random pixels within the overcast sky area.

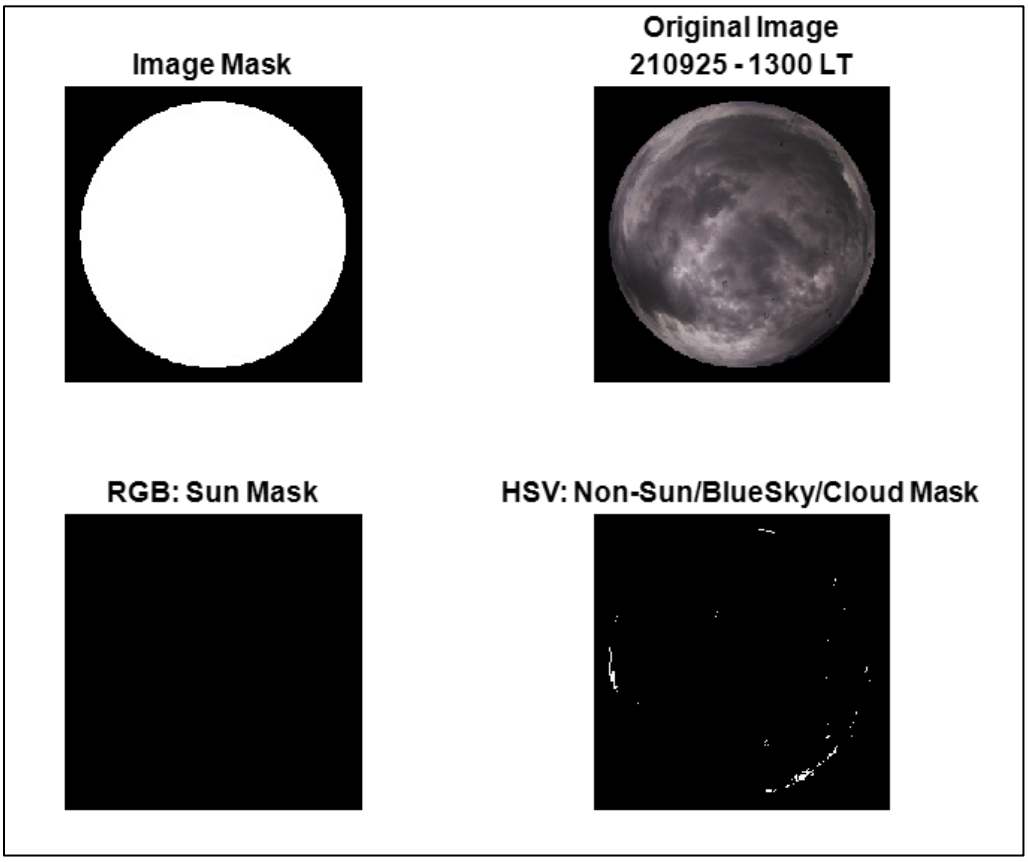

Fig. C-1 OVC results example from 2021 September 25, 1300 LT

The CLR example shown in Fig. C-2 is from 2021 September 14, 1300 LT. There is no difference in the image mask (upper left) from Fig. C-1; however, this case's original image (upper right) shows no clouds within the WSI region. The sun mask (lower left) isolates the sun, corona, and etchings from the WSI lens material. The HSV image zeros (black pixels) represent the WSI rectangle frame, sun mask area, and an upside-down teardrop lens artifact caused by the sun's passage through the fisheye lens.

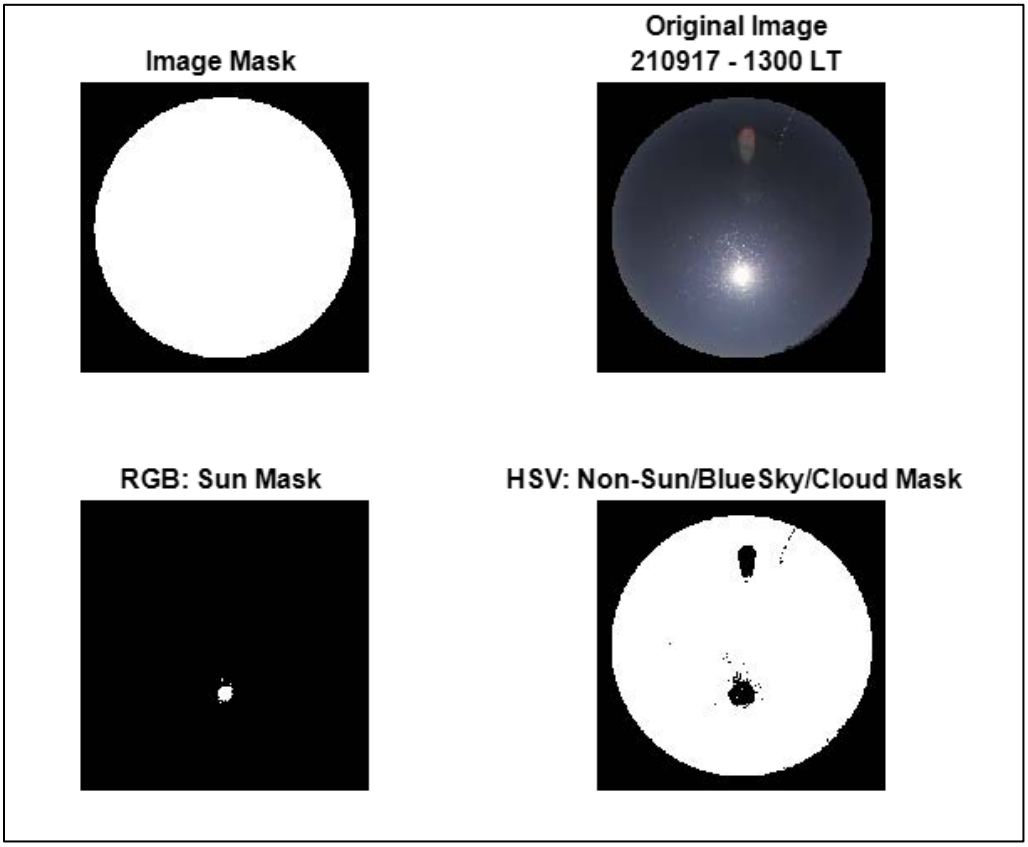

Fig. C-2 CLR results example from 2021 September 14, 1300 LT

The PC example (Fig. C-3) is from 2021 October 1, 1300 LT. The image mask (upper left) is consistent with the previous examples. The original image (upper right) shows a mix of clouds and blue sky. Since the clouds cover the sun, there are no white (value is 1) pixels in the sun mask (lower left). In the HSV image, clouds are zeroed (black pixels) and the blue sky area is white. Note that the white areas include shapes close to the horizon.

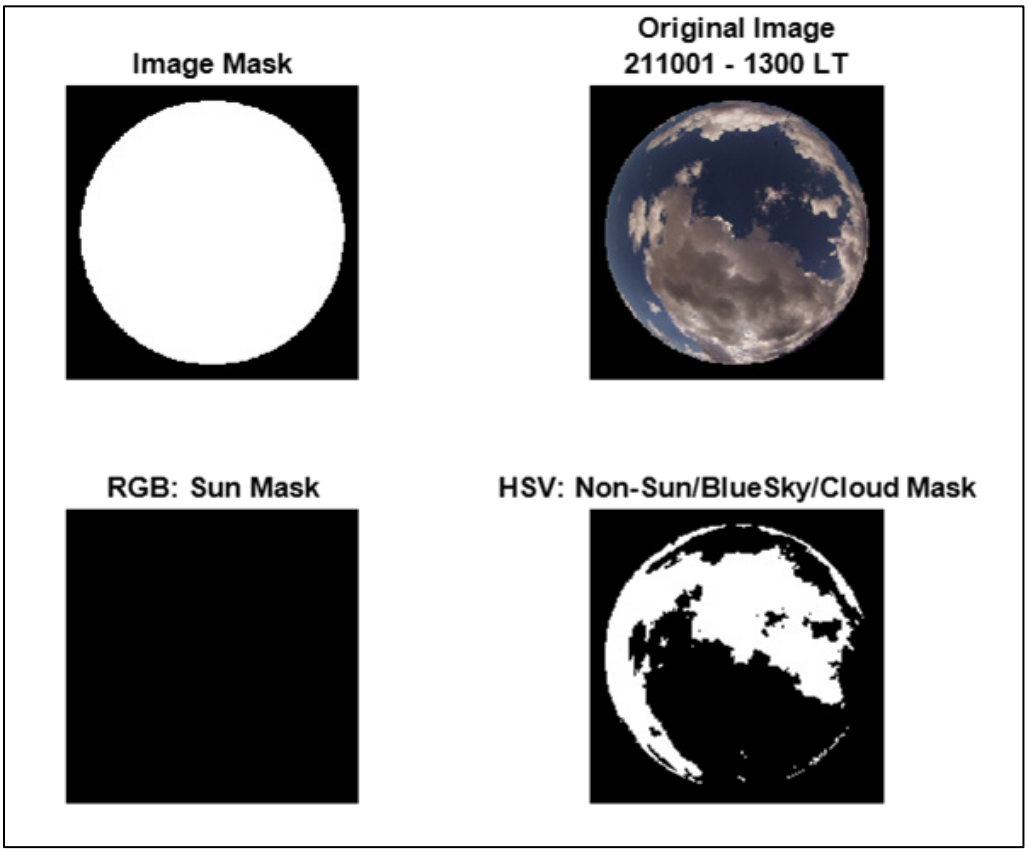

Fig. C-3 PC results example from 2021 October 1, 1300 LT

C.2 RGB and HSV Results: All Cases by Sky Type

Figures C-4 through C-6 show results from the full 15 cases, separated into their respective sky types.

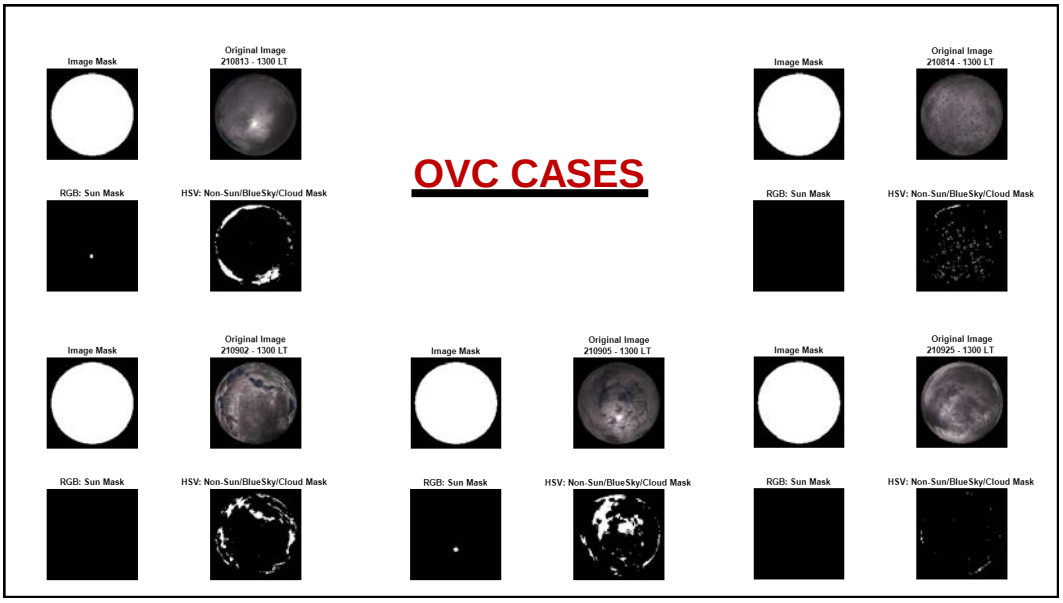

Fig. C-4 Five OVC case image results

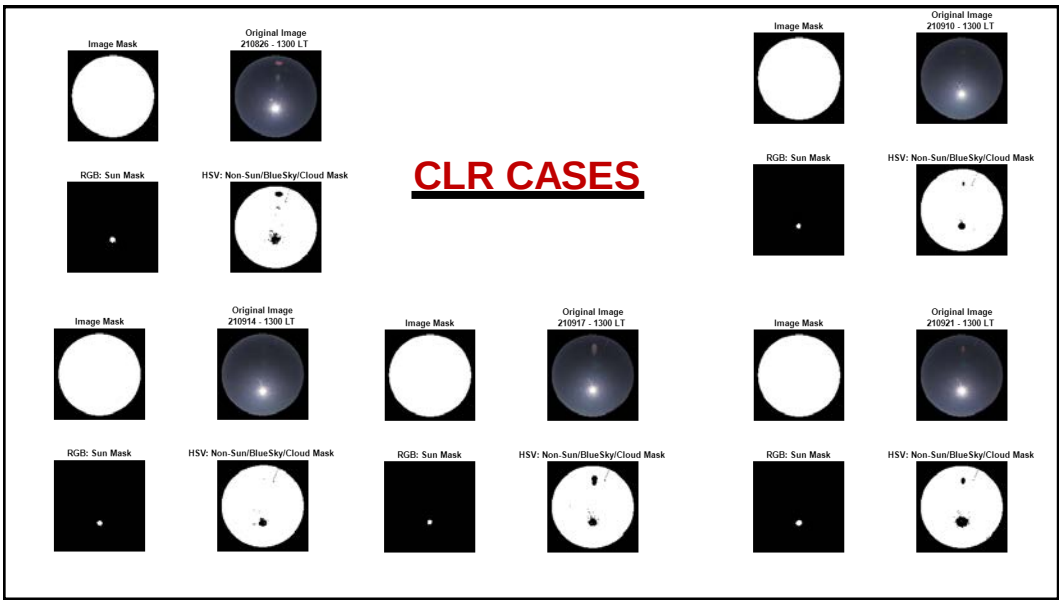

Fig. C-5 Five CLR case image results

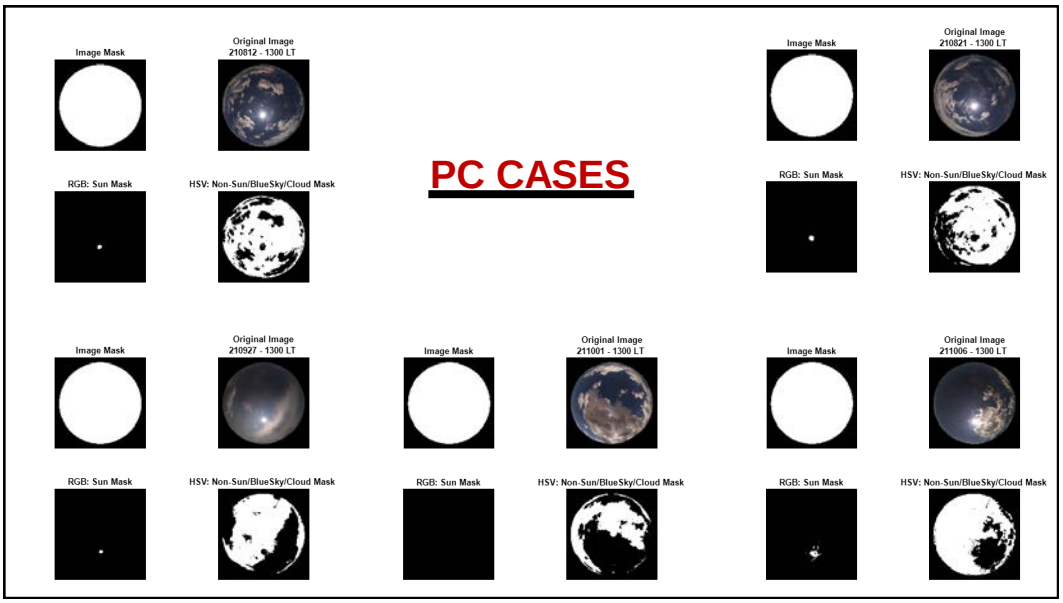

Fig. C-6 Five PC case image results

C.3 RGB and HSV Results: Tabulated Results of All Cases

Pixel counts founded from the circular WSI image were converted into percentage of the image values. As reported in Table C-1, the total circular WSI image count was 666,999 pixels. After grouping the cases by sky type, the major image elements of each WSI image were tallied (in percent), followed by their sky totals (also in percent). The Meteorological Measurement Tripod (MMT) ground sensor values were not used in the totals, except where noted. Sky totals were well within the accepted 3% non-sky elements determined by this study. Table C-1 is an extension of Section 4.

Table C-1 Numerical results of calculated vs. total pixel count by sky type

Date	Local Time	Total WSI	Sun	Blue Sky	MMT	Calc Cloud Cover	Std Total Sky	Calculated Total Sky (no MMT)	Total Sky Difference (Calc - Std)	Calculated Total Sky with MMT	MMT: Total Sky Difference (Calc - Std)
YYMMDD	Hrs	Pixels	Percent	Percent	Percent	Percent	Percent	Percent	Percent	Percent	Percent
								OVC=(S+B+C)		OVC=(S+B+C+M)	
210813	1300	666999	0.1909	9.8964	0.1840	90.1036	100.0	100.1909	**0.1909**	100.3748	0.3748
210814	1300	666999	0.0000	2.9297	0.0865	97.0703	100.0	100.0000	**0.0000**	100.0865	0.0865
210902	1300	666999	0.0000	10.7633	0.2894	89.2367	100.0	100.0000	**0.0000**	100.2894	0.2894
210905	1300	666999	0.3096	17.5658	0.0942	82.4342	100.0	100.3096	**0.3096**	100.4037	0.4037
210925	1300	666999	0.0000	0.6492	0.0820	99.3508	100.0	100.0000	**0.0000**	100.0820	0.0820
								CLR=(S+B+C)		CLR=(S+B+C+M)	
210826	1300	666999	0.4637	98.0637	1.8604	1.9363	100.0	100.4637	**0.4637**	102.3241	2.3241
210910	1300	666999	0.3183	99.1745	1.8499	0.8255	100.0	100.3183	**0.3183**	102.1682	2.1682
210914	1300	666999	0.3937	98.7538	1.8244	1.2462	100.0	100.3937	**0.3937**	102.2181	2.2181
210917	1300	666999	0.3789	98.0813	1.8622	1.9187	100.0	100.3789	**0.3789**	102.2411	2.2411
210921	1300	666999	0.5322	97.5288	1.8690	2.4712	100.0	100.5322	**0.5322**	102.4012	2.4012
								PC=(S+B+C)		PC=(S+B+C+M)	
210812	1300	666999	0.2684	74.1307	1.7664	25.8693	100.0	100.2684	**0.2684**	102.0348	2.0348
210821	1300	666999	0.3855	72.3054	1.9249	27.6946	100.0	100.3855	**0.3855**	102.3103	2.3103
210927	1300	666999	0.2181	63.6731	1.4220	36.3269	100.0	100.2181	**0.2181**	101.6402	1.6402
211001	1300	666999	0.0030	44.1639	1.2313	55.8361	100.0	100.0030	**0.0030**	101.2343	1.2343
211006	1300	666999	0.9486	76.6078	1.7978	23.3922	100.0	100.9486	**0.9486**	102.7463	2.7463

List of Symbols, Abbreviations, and Acronyms

ARL	Army Research Laboratory
BKN	broken
CLR	clear
DEVCOM	US Army Combat Capabilities Development Command
GLOBE	Global Learning and Observation to Benefit the Environment
HSV	hue, saturation, and value
LT	local time
Max	maximum
MDT	mountain daylight time
Min	minimum
MMT	Meteorological Measurement Tripod
MST	mountain standard time
OVC	overcast
PC	partly cloudy
PV	photovoltaic
RGB	red, green, and blue
ROI	region of interest
SCT	scattered
Std	standard
WSI	Whole Sky Imager
X	surface-based obscuring phenomena